

FLUX RECONSTRUCTION FOR GOAL-ORIENTED A POSTERIORI ESTIMATION

MARTIN LICHT AND MATTHIAS MAIER

ABSTRACT. We propose a new heuristic goal-oriented a posteriori error estimator that connects the dual weighted residual method with equilibrated a posteriori error estimation. Our numerical experiments demonstrate the practical reliability of the error estimator, confirming theoretical predictions, as well as optimally convergent adaptivity even over singular domains and coarse meshes. The central algorithm is a localized flux reconstruction, which has been implemented in the finite element library deal.II. For a solid preparation we assess the performance of the equilibrated a posteriori error estimator of the energy norm in numerical experiments. Moreover, we give what seems to be first rigorous discussion in the numerical literature of localized flux reconstruction over quadrilateral meshes with hanging nodes.

1. INTRODUCTION

A *posteriori error estimation* is an important concept in assessing the accuracy of finite element methods for partial differential equations. Many a posteriori error estimators not only bound the global error but also indicate the local contributions of the approximation error. Thus, they are fundamental to *adaptive finite element methods* based on local mesh refinement. The overall importance of a posteriori estimation is reflected by the large corpus of literature on this topic (see [3, 30, 34] and the references therein). Typically, convergence is shown with respect to global energy norms. In many applications, however, we are more interested in approximating a *quantity of interest*, assumed (for simplicity) to be a linear functional of the true solution. *Goal-oriented a posteriori error estimates* bound or approximate the error in the quantity of interest.

Equilibrated error estimators are provably reliable and are considered to be among the most efficient residual-based error estimators [1]. They come in several variants, whose common idea is to compute error estimates by solving localized subproblems with data constructed from the global right-hand sides and the approximate solution. In this article, we focus on the family of equilibrated error estimators based on solving local divergence equations over patches around mesh nodes (see also [19, 22, 23, 13, 12, 16, 21]). These error estimators are reliable, constant-free, and computable.

The contributions of this article are both theoretical and experimental in nature. We report on an equilibrated a posteriori error estimators implemented in

2000 *Mathematics Subject Classification.* 65N30.

Key words and phrases. A posteriori error estimation, dual weighted residual method, equilibrated error estimation, flux reconstruction, goal functional, quantity of interest.

This research was supported by the European Research Council through the FP7-IDEAS-ERC Starting Grant scheme, project 278011 STUCCOFIELDS.

the finite element software library deal.II [5]. Our experiments with the Poisson problem show a typical overestimation of the energy error by 30–70% and optimal convergence of adaptive finite element methods, in accordance with similar findings in the numerical literature [16].

An innovation at this point is our exposition of the construction and well-posedness of the local divergence equations in the finite element flux reconstruction; see Lemma 1. To the best of our knowledge, we give the first such account for the case of quadrilateral meshes with hanging nodes. Since deal.II and many other finite element software libraries employ this class of meshes, this article closes a practically relevant gap in the literature. We also remark that all our results are stated for mixed boundary conditions and in arbitrary dimension.

These theoretical and practical results prepare our successive contributions to goal-oriented a posteriori error estimation. We develop and assess a new heuristic goal-oriented error estimator, combining the basic idea of the dual weighted residual method [8] with techniques of equilibrated a posteriori error estimation.

Our new error estimator requires finite element approximations for the original (primal) problem and the adjoint (dual) problem associated with the goal functional. In addition, it needs localized flux reconstructions for both problems. We show that our error estimator coincides with the true error in the quantity of interest up to a perturbation that depends on approximation errors of mixed finite element methods for the primal and the dual problem. The latter term typically converges with higher order than the error estimator, depending on the regularity of the domain. This is in accordance with our computational experiments, which demonstrate the practical reliability of the new estimator both on regular and singular domains. We furthermore observe optimal convergence of a corresponding goal-oriented adaptive finite element method.

Computational experiments compare our error estimator with a dual weighted residual estimator and a goal-oriented error estimator proposed by Mozolevski and Prudhomme [25]. The former leads to an optimally convergent goal-oriented adaptive finite element method but significantly underestimates the error on coarse triangulations and on singular domains. The latter gives reliable error estimates in practice but displays suboptimal adaptive convergence rates in our numerical experiments, which we attribute to oscillatory behavior. Our new error estimator consistently avoids those problems.

The remainder of this article is structured as follows. In Section 2 we review the analytical background. In Section 3 we give a concise introduction to the method of the hypercircle for the Poisson problem. Subsequently, Section 4 describes the localized flux reconstruction. Section 5 discusses goal-oriented a posteriori error estimation. Finally, Section 6 presents a number of numerical experiments. A conclusive summary follows in Section 7.

2. ANALYTICAL BACKGROUND

In this section we recall a number of basic function spaces and some fundamental results. Throughout the paper we let $\Omega \subset \mathbb{R}^n$ be a fixed bounded Lipschitz domain. Furthermore, we fix a pair Γ_D and Γ_N of relatively open subsets of $\partial\Omega$ such that $\partial\Omega = \bar{\Gamma}_D \cup \bar{\Gamma}_N$ and $\Gamma_D \cap \Gamma_N = \emptyset$.

Let $L^p(\Omega)$ denote the Lebesgue space over Ω with exponent $p \in [1, \infty]$. These spaces are equipped with the canonical L^p norms $\|\cdot\|_{L^p}$. In the case $p = 2$, this norm

is induced by a canonical scalar product $\langle \cdot, \cdot \rangle_{L^2}$. Furthermore, $\mathbf{L}^p(\Omega) = L^p(\Omega)^n$ denotes the Banach space of vector fields over Ω with coefficients in $L^p(\Omega)$. This space is equipped with the canonical norm $\| \cdot \|_{\mathbf{L}^p}$. Again, this norm is induced by a scalar product $\langle \cdot, \cdot \rangle_{\mathbf{L}^2}$ in the case $p = 2$.

We call a matrix field $A \in L^\infty(\Omega)^{n \times n}$ an *admissible metric tensor* if A is symmetric and invertible almost everywhere over Ω with $A^{-1} \in L^\infty(\Omega)^{n \times n}$. Every such A induces a bounded isomorphism $A : \mathbf{L}^2(\Omega) \rightarrow \mathbf{L}^2(\Omega)$ by multiplication and induces the A -scalar product $\langle \sigma, \tau \rangle_A := \langle \sigma, \tau \rangle_{\mathbf{L}_A^2(\Omega)} := \langle \sigma, A\tau \rangle_{\mathbf{L}^2}$ over $\mathbf{L}^2(\Omega)$, which is equivalent to the canonical scalar product on $\mathbf{L}^2(\Omega)$.

We write $H^1(\Omega)$ for the first-order Sobolev space over Ω , and we let $\mathbf{H}(\Omega, \text{div})$ denote the subspace of $\mathbf{L}^2(\Omega)$ whose members have their divergences (a priori taken in the sense of distributions) in $L^2(\Omega)$. We equip $H^1(\Omega)$ and $\mathbf{H}(\Omega, \text{div})$ with the canonical scalar products. We let $H^1(\Omega, \Gamma_D)$ be the closed subspace of $H^1(\Omega)$ whose members have vanishing trace along Γ_D . Similarly, $\mathbf{H}(\Omega, \Gamma_N, \text{div})$ shall denote the closed subspace of $\mathbf{H}(\Omega, \text{div})$ whose members have vanishing normal trace along Γ_N . The integration-by-parts formula

$$(1) \quad \int_{\Omega} \langle \nabla v, \tau \rangle \, dx + \int_{\Omega} \langle v, \text{div} \tau \rangle \, dx = \oint_{\partial\Omega} \text{tr} v \cdot \text{tr}_N \tau \, ds$$

holds for every $v \in H^1(\Omega)$ and $\tau \in \mathbf{H}(\Omega, \text{div})$. Here, the boundary integral is understood in the generalized sense and vanishes if $v \in H^1(\Omega, \Gamma_D)$ and $\tau \in \mathbf{H}(\Omega, \Gamma_N, \text{div})$. We let $H^{-1}(\Omega, \Gamma_N) := H^1(\Omega, \Gamma_D)^*$ denote the topological dual space of $H^1(\Omega, \Gamma_D)$. This is again a Hilbert space equipped with the canonical operator norm. We also write $\langle \cdot, \cdot \rangle$ for the distributional pairing between $H^1(\Omega, \Gamma_D)$ and $H^{-1}(\Omega, \Gamma_N)$. We have a bounded operator

$$(2) \quad \nabla : H^1(\Omega, \Gamma_D) \rightarrow \mathbf{L}_A^2(\Omega), \quad v \mapsto \nabla v,$$

whose dual is given by the bounded operator

$$(3) \quad -\text{div}_{\Omega, \Gamma_N} : \mathbf{L}_A^2(\Omega) \rightarrow H^{-1}(\Omega, \Gamma_N), \quad \tau \mapsto \langle \tau, \nabla \cdot \rangle_A.$$

This extension of the divergence operator to $\mathbf{L}^2(\Omega)$ commutes with the natural embeddings. We have the generalized integration-by-parts formula

$$(4) \quad \langle \tau, \nabla v \rangle_A = \langle \text{div}_{\Omega, \Gamma_N} \tau, v \rangle, \quad \tau \in \mathbf{L}^2(\Omega), \quad v \in H^1(\Omega, \Gamma_D).$$

For our discussion of the Poisson problem, we let $\mathcal{H}(\Omega, \Gamma_D)$ denote the locally constant functions contained in $H^1(\Omega, \Gamma_D)$. This is just the span of the indicator functions of those connected components of Ω that do not touch Γ_D . We let $\mathcal{H}_{\Omega, \Gamma_D} v$ denote the L^2 -orthogonal projection of any $v \in L^2(\Omega)$ onto $\mathcal{H}(\Omega, \Gamma_D)$. The linear mapping $\mathcal{H}_{\Omega, \Gamma_D}$ extends naturally to $H_N^{-1}(\Omega)$.

Remark 1. On a connected domain, the space $\mathcal{H}(\Omega, \Gamma_D)$ will be either the span of the constant function or trivial, depending on whether Γ_D is empty or not. This notation will come in handy later in Section 4, where we consider local divergence equations over varying subdomains of Ω with varying boundary conditions.

With these definitions in mind, we state the following Poincaré-Friedrichs inequalities. There exists a constant $C_A^{\text{PF}} > 0$, depending only on Ω , Γ_D and A , such that for every $v \in H^1(\Omega, \Gamma_D)$ we have

$$(5) \quad \|v - \mathcal{H}_{\Omega, \Gamma_D} v\|_{L^2} \leq C_A^{\text{PF}} \|\nabla v\|_A.$$

On the other hand, for every $F \in H^{-1}(\Omega, \Gamma_N)$ there exists $\tau \in \mathbf{L}^2(\Omega)$ such that

$$(6) \quad -\operatorname{div}_{\Omega, \Gamma_N} \tau = F - \mathcal{H}_{\Omega, \Gamma_D} F, \quad \|\tau\|_A \leq C_A^{\text{PF}} \|F - \mathcal{H}_{\Omega, \Gamma_D} F\|_{H^{-1}(\Omega, \Gamma_N)}.$$

Note that $F \in L^2(\Omega)$ implies $\tau \in \mathbf{H}(\Omega, \Gamma_N, \operatorname{div})$ in (6).

Finally, a modicum of Hodge theory is utilized throughout this article. We set

$$(7) \quad \mathbf{X}(\Omega, \Gamma_N, A) := \nabla (H^1(\Omega, \Gamma_D))^{\perp A} = \{\tau \in \mathbf{L}^2(\Omega) : \operatorname{div}_{\Omega, \Gamma_N} A\tau = 0\}.$$

This is precisely the Hilbert space of those $\tau \in \mathbf{L}^2(\Omega)$ for which $A\tau \in \mathbf{H}(\Omega, \operatorname{div})$ has vanishing divergence and homogeneous normal trace along Γ_N . Basic functional analysis gives the A -orthogonal *Hodge-Helmholtz decomposition*

$$(8) \quad \mathbf{L}^2(\Omega) = \nabla H^1(\Omega, \Gamma_D) \oplus_A \mathbf{X}(\Omega, \Gamma_N, A).$$

3. ERROR ESTIMATES FOR THE POISSON PROBLEM

In this section we outline reliable error estimates for approximate solutions of the Poisson problem based on the hypercircle identity and its generalizations. Here, our results rely on techniques in functional analysis, and no further details on the method of approximation are assumed at this point.

3.1. Model Problem. Our object of discussion is the partial differential equation

$$(9) \quad -\operatorname{div}_{\Omega, \Gamma_N} A\nabla u = F - \mathcal{H}_{\Omega, \Gamma_D} F, \quad u \perp \mathcal{H}(\Omega, \Gamma_D),$$

where $F \in H^{-1}(\Omega, \Gamma_N)$ is the data, $A \in L^\infty(\Omega)^{n \times n}$ is a fixed admissible metric tensor, and the function $u \in H^1(\Omega, \Gamma_D)$ is the unknown. The Poisson equation in above form is precisely the weak formulation that characterizes u by requiring

$$(10a) \quad \langle \nabla u, \nabla v \rangle_A = F(v - \mathcal{H}_{\Omega, \Gamma_D} v), \quad v \in H^1(\Omega, \Gamma_D),$$

$$(10b) \quad u \perp \mathcal{H}(\Omega, \Gamma_D).$$

The well-posedness of this problem follows from standard elliptic regularity theory. For every right-hand side $F \in H^{-1}(\Omega, \Gamma_N)$ there exists a unique solution $u \in H^1(\Omega, \Gamma_D)$ of (9), and we can estimate

$$(11) \quad \|u\|_{L^2} \leq (C_A^{\text{PF}})^2 \|F\|_{H^{-1}(\Omega, \Gamma_N)}, \quad \|\nabla u\|_A \leq C_A^{\text{PF}} \|F\|_{H^{-1}(\Omega, \Gamma_N)}.$$

Throughout this section, a candidate approximation $u_h \in H^1(\Omega, \Gamma_D)$ is assumed to be already known. We want to compute information about the error $u - u_h$, such as bounds in Sobolev norms. In our prospective applications, u_h is computed with a Galerkin method for the Poisson problem, but the exact solution u is unknown.

Remark 2. The Poisson equation is often studied only for square-integrable right-hand sides $F \in L^2(\Omega)$, so that $\nabla u \in H(\Omega, \Gamma_N, \operatorname{div})$ by definition. We consider a distributional right-hand side in $H^{-1}(\Omega, \Gamma_N)$ in this article, which allows for a neat formalism for inhomogeneous mixed boundary conditions.

3.2. Reliable Error Estimation. We derive reliable error estimates in the energy seminorm via the *hypercircle method*. For that purpose we assume that $\sigma_h \in \mathbf{L}^2(\Omega)$ is any solution of the *flux equation*

$$(12) \quad -\operatorname{div}_{\Omega, \Gamma_N} A\sigma_h = F - \mathcal{H}_{\Omega, \Gamma_D} F.$$

The availability of such σ_h is stipulated for the time being. The specific auxiliary computations that solve the flux equation (12) in applications will be examined later in this article.

Under this assumption, it is elementary to derive

$$\|\nabla u_h - \sigma_h\|_A^2 = \|\nabla u_h - \nabla u\|_A^2 + \|\nabla u - \sigma_h\|_A^2 + 2 \langle \nabla(u_h - u), A\nabla u - A\sigma_h \rangle_{\mathbf{L}^2}.$$

Since σ_h solves the flux equation (12), integration by parts yields

$$\begin{aligned} \langle \nabla(u_h - u), A\nabla u - A\sigma_h \rangle_{\mathbf{L}^2} &= \langle u_h - u, \operatorname{div}_{\Omega, \Gamma_N} A\nabla u - \operatorname{div}_{\Omega, \Gamma_N} A\sigma_h \rangle_{\mathbf{L}^2} \\ &= \langle u_h - u, (\operatorname{Id} - \mathcal{H}_{\Omega, \Gamma_D})F - (\operatorname{Id} - \mathcal{H}_{\Omega, \Gamma_D})F \rangle \\ &= 0. \end{aligned}$$

Thus we obtain what is known as the *hypercircle identity*:

$$(13) \quad \|\nabla u_h - \sigma_h\|_A^2 = \|\nabla u_h - \nabla u\|_A^2 + \|\nabla u - \sigma_h\|_A^2.$$

We note that the left-hand side of (13) is given explicitly in terms of entities that are computable by assumption. We thus get the simple and computable estimate

$$(14) \quad \|\nabla u_h - \sigma_h\|_A \geq \|\nabla u_h - \nabla u\|_A.$$

This bounds the error $u - u_h$ in the energy seminorm, which is the dominant term of the full H^1 error norm in typical applications, in a manner computable in terms of only ∇u_h and σ_h .

Remark 3. Any computable estimate for $\nabla u - \nabla u_h$ in the A -norm gives an estimate for $u - u_h$ in the L^2 -norm, as follows by the Poincaré-Friedrichs inequality (5). This estimate is computable if a bound for the Poincaré-Friedrichs constant C_A^{PF} can be computed. Such estimates are not within the scope of this article, but we refer to the literature [27] for research in that direction.

Remark 4. The error identity (13) goes back to the seminal research of Prager and Synge in the field of mathematical elasticity [29] and is thus known as *Prager-Synge identity* in the literature. The underlying technique is also called *hypercircle method* because, as a consequence of Thales' theorem in Hilbert spaces, the vector fields ∇u , ∇u_h , and σ_h are located on a common hypercircle in the space of square-integrable vector fields [20, 31, 32]. Furthermore, the technique is known as *two-energy principle* because it compares an approximate minimizer of the Poisson energy to an approximate minimizer of its conjugate energy [11]. In the context of a posteriori error estimates, Equation (14) is called a *constant-free* error estimate because it does not involve generic or uncertain constants, unlike, say, the classical residual error estimator [33]. We also bring to attention that *functional-type error estimates* [28] utilize similar techniques.

3.3. Efficiency. Having established the reliable error estimate (14), we now discuss its efficiency. The latter depends, broadly speaking, on the “efficiency” of σ_h as a solution to the flux equation. We first recall that

$$\operatorname{div}_{\Omega, \Gamma_N} A(\nabla u - \sigma_h) = F - F = 0.$$

Now $\nabla u - \sigma_h \in \mathbf{X}(\Omega, \Gamma_N, A)$ follows from the the definition of $\mathbf{X}(\Omega, \Gamma_N, A)$ in Equation (7). Thus there exists a unique $\theta_h := \nabla u - \sigma_h \in \mathbf{X}(\Omega, \Gamma_N, A)$ such that we have the A -orthogonal decomposition

$$(15) \quad \sigma_h = \nabla u + \theta_h.$$

Via the Pythagorean theorem, we readily compute that

$$\|\nabla u_h - \sigma_h\|_A^2 = \|\nabla u_h - \nabla u - \theta_h\|_A^2 = \|\nabla u_h - \nabla u\|_A^2 + \|\theta_h\|_A^2.$$

We quantify the efficiency of the error estimate (14) as

$$(16) \quad \frac{\|\nabla u_h - \sigma_h\|_A^2}{\|\nabla u_h - \nabla u\|_A^2} = 1 + \frac{\|\theta_h\|_A^2}{\|\nabla u_h - \nabla u\|_A^2}.$$

We conclude that the ‘‘efficiency’’ of the flux reconstruction determines the efficiency of the error estimate: the rigorously reliable error estimate (14) will be the sharper, the smaller the norm of $\theta_h = \sigma_h - \nabla u$. This generally depends on the specific construction of σ_h in applications; for a specific construction, a bound of $\|\theta_h\|_A$ in terms of $\|\nabla u_h - \nabla u\|_A$ will be given later in this article.

Remark 5. The relevance of the Hodge-Helmholtz decomposition for equilibrated error estimation is recognized in the published literature [16]. Some simple postprocessing techniques are known to effectively improve the approximation properties of the numerically computed flux and thus the efficiency of the resulting error estimates.

3.4. Approximate Flux Reconstruction. In many applications it may not be computationally feasible to construct a vector field $\sigma_h \in \mathbf{L}^2(\Omega)$ solving the flux equation (12) exactly. Instead, we may have a vector field $\sigma_h \in \mathbf{L}^2(\Omega)$ that solves an *approximate flux equation*

$$(17) \quad -\operatorname{div}_{\Omega, \Gamma_N} A \sigma_h = F_h - \mathcal{H}_{\Omega, \Gamma_D} F_h$$

for some right-hand side $F_h \in H^{-1}(\Omega, \Gamma_N)$. In typical applications, F_h is a given approximation of F and the variable σ_h is constructed from F_h as an approximate solution of the original flux equation.

For a reliable estimate of the A -norm of $\nabla u - \nabla u_h$, we formally introduce the unique solution $\hat{u} \in H^1(\Omega, \Gamma_D)$ of the *approximate Poisson problem*

$$-\operatorname{div}_{\Omega, \Gamma_N} A \nabla \hat{u} = F_h - \mathcal{H}_{\Omega, \Gamma_D} F_h, \quad \hat{u} \perp \mathcal{H}(\Omega, \Gamma_D).$$

The triangle inequality states

$$\|\nabla u - \nabla u_h\|_A \leq \|\nabla u - \nabla \hat{u}\|_A + \|\nabla \hat{u} - \nabla u_h\|_A.$$

On the one hand, the Poincaré-Friedrichs inequality (6) gives

$$\|\nabla u - \nabla \hat{u}\|_A \leq C_A^{\text{PF}} \|F - F_h\|_{H^{-1}(\Omega, \Gamma_N)}.$$

On the other hand, when considering u_h as an approximation to \hat{u} , the classical hypercircle identity gives

$$\|\nabla \hat{u} - \nabla u_h\|_A \leq \|\sigma_h - \nabla u_h\|_A.$$

In summary, we get the reliable error estimate

$$(18) \quad \|\nabla u - \nabla u_h\|_A \leq C_A^{\text{PF}} \|F - F_h\|_{H^{-1}(\Omega, \Gamma_N)} + \|\sigma_h - \nabla u_h\|_A.$$

If $A \sigma_h \in H_N(\operatorname{div}, \Omega)$ and $F \in L^2(\Omega)$, then the negative Sobolev norms in (18) can be bounded by the L^2 -norm of $F - F_h$. The entire estimate is fully computable provided that an estimate for the Poincaré-Friedrichs constant is known.

Whereas this addresses the reliability, we also address the efficiency of (18). This generally depends on the Hodge-Helmholtz decomposition of the flux variable σ_h , whose component in $\mathbf{X}(\Omega, \Gamma_N, A)$ we desire to be as small as possible, and on the consistency error $F_h - F$. By construction, there exists $\hat{\theta}_h \in \mathbf{X}(\Omega, \Gamma_N, A)$ with

$$\hat{\theta}_h = \sigma_h - \nabla \hat{u}.$$

The efficiency of the error estimate (18) is the right-hand side of that inequality divided by the true error $\|\nabla u - \nabla u_h\|_A$. With the observation

$$\begin{aligned} \|\sigma_h - \nabla u_h\|_A &\leq \|\widehat{\theta}_h\|_A + \|\nabla \widehat{u} - \nabla u\|_A + \|\nabla u - \nabla u_h\|_A \\ &\leq \|\widehat{\theta}_h\|_A + C_A^{\text{PF}} \|F - F_h\|_{H^{-1}(\Omega, \Gamma_N)} + \|\nabla u - \nabla u_h\|_A \end{aligned}$$

we observe that the efficiency of (18) satisfies the computable bounds

$$\begin{aligned} (19) \quad 1 &\leq C_A^{\text{PF}} \frac{\|F - F_h\|_{H^{-1}(\Omega, \Gamma_N)}}{\|\nabla u - \nabla u_h\|_A} + \frac{\|\sigma_h - \nabla u_h\|_A}{\|\nabla u - \nabla u_h\|_A} \\ &\leq 1 + 2C_A^{\text{PF}} \frac{\|F - F_h\|_{H^{-1}(\Omega, \Gamma_N)}}{\|\nabla u - \nabla u_h\|_A} + \frac{\|\widehat{\theta}_h\|_A}{\|\nabla u - \nabla u_h\|_A}. \end{aligned}$$

We rephrase this result in a suggestive manner: the generalized estimate (19) is efficient provided that σ_h is an efficient solution to an efficient approximation of the original flux equation. Note that (16) is recovered in the special case $F = F_h$.

Remark 6. In many applications, not only the true right-hand side F is approximated by an approximate right-hand side F_h , but also the true coefficient A is approximated by an approximate coefficient A_h assumed to be an admissible metric tensor. Suppose that $\sigma'_h \in \mathbf{L}^2(\Omega)$ solves the approximate flux equation

$$-\operatorname{div}_{\Omega, \Gamma_N} A_h \sigma'_h = F_h - \mathcal{H}_{\Omega, \Gamma_D} F_h$$

with the approximate coefficient A_h . Via the simple observation $A_h = A(A^{-1}A_h)$ we can apply the error estimate (19) with the flux variable $\sigma_h = A^{-1}A_h \sigma'_h$. So the case of approximate coefficients can be reduced to the case of exact coefficients.

3.5. Residual Flux Reconstruction. In the next section, it will be conceptually helpful to use a variation of the flux equation (12) (or (17), respectively). Suppose that $F_h \in H^{-1}(\Omega, \Gamma_N)$ is any approximate right-hand side. We define the *residual* $r_h \in H^{-1}(\Omega, \Gamma_N)$ by

$$(20) \quad r_h = F_h - \mathcal{H}_{\Omega, \Gamma_D} F_h + \operatorname{div}_{\Omega, \Gamma_N} A \nabla u_h.$$

Given any solution $\varrho_h \in \mathbf{L}^2(\Omega)$ of the *residual flux equation*

$$(21) \quad -\operatorname{div}_{\Omega, \Gamma_N} A \varrho_h = r_h,$$

the vector field $\sigma_h = \varrho_h + \nabla u_h$ solves the approximate flux equation (17). In many applications it is easier to first solve the residual flux equation (21) with right-hand side r_h and derive σ_h in the aforementioned manner, rather than directly solving the flux equation with the effective right-hand side F_h . This is intuitive: the approximate solution u_h typically depends on the right-hand side F_h and thus contains additional information on F_h that can be used in the flux reconstruction.

4. FINITE ELEMENT FLUX RECONSTRUCTION

In this section we discuss the implementation of a local flux reconstruction over quadrilateral finite element meshes with hanging nodes. In particular, we give a formal proof of the well-posedness of the local problems (see Lemma 1), and we keep the discussion independent of the spatial dimension. For the context and motivation of this section, we recall that the abstract error estimates of the previous section require a solution of the flux equation (12), or equivalently, of the residual

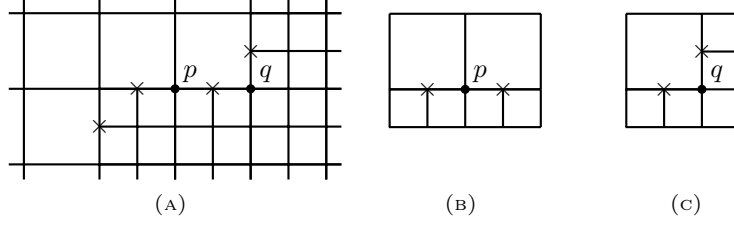


FIGURE 1. A quadrilateral mesh (a) with hanging nodes (\times) and reconstructed patches around nodes $p \in \mathcal{N}_h^I$ (b) and $q \in \mathcal{N}_h^I$ (c).

flux equation (21). The localized flux reconstruction efficiently computes such a solution in finite element spaces.

The main ideas of the local flux reconstruction can be found in the literature for other types of meshes [12]. Classical finite element over quadrilateral non-conforming meshes are described in [14].

4.1. Finite Element Spaces. Let Ω_h be a partition of a polygonal domain Ω into convex, non-degenerate quadrilaterals. We relax the usual *form regularity* by allowing *hanging nodes* of at most one level. Let \mathcal{N}_h be the set of nodes of the partition Ω_h and let $\mathcal{N}_h^I \cup \mathcal{N}_h^H$ be a partition of \mathcal{N}_h into unconstrained nodes \mathcal{N}_h^I and hanging nodes \mathcal{N}_h^H ; see Figure 1. In addition, we let $\mathcal{N}_h^I(K)$ be the set of nodes in \mathcal{N}_h^I that are contained in an element $K \in \Omega_h$. We write \mathcal{F}_h for the set of faces of the quadrilaterals in the partition. We let \mathcal{F}_h^I denote the subset of \mathcal{F}_h whose members are not contained in any other member of \mathcal{F}_h , and we let $\mathcal{F}_h^H := \mathcal{F}_h \setminus \mathcal{F}_h^I$.

We let $\Gamma_D \subseteq \partial\Omega$ be a subset of the boundary that is the union of faces of the partition. We also let $\Gamma_N \subseteq \partial\Omega$ be the essential complement of Γ_D in $\partial\Omega$, which is again a union of faces of the partition.

We let \widehat{K} denote the unit square, and for every full-dimensional cell $K \in \Omega_h$ we let $\Psi_K : \widehat{K} \rightarrow K$ be a fixed affine reference transformation. We let $C_h > 0$ be the *shape-constant* of the partition Ω_h , which is defined as the minimal non-negative number satisfying $\|\mathbf{D}\Psi_K\|_{L^\infty(\widehat{K})} < C_h$ and $\|\mathbf{D}\Psi_K^{-1}\|_{L^\infty(K)} < C_h$ for every full-dimensional quadrilateral $K \in \Omega_h$.

We define several finite element spaces, beginning with scalar functions. We write $\mathbf{Q}^r(K)$ and $\mathbf{Q}^r(F)$ for the space of polynomials over any full-dimensional cell $K \in \Omega_h$ and any codimension-one face $F \in \mathcal{F}_h$ of the partition, respectively, with maximum degree r in each variable. We let $\mathbf{Q}_{-1}^r(\Omega_h)$ denote the space of functions that are piecewise polynomials of degree at most r in each variable with respect to the partition Ω_h . We have

$$\mathbf{Q}_{-1}^r(\Omega_h) := \sum_{K \in \Omega_h} \mathbf{Q}^r(K).$$

We define $\mathbf{Q}^r(\Omega_h) := H^1(\Omega) \cap \mathbf{Q}_{-1}^r(\Omega_h)$ as the H^1 -conforming subspace of $\mathbf{Q}_{-1}^r(\Omega_h)$, and we define $\mathbf{Q}^r(\Omega_h, \Gamma_D) := H^1(\Omega, \Gamma_D) \cap \mathbf{Q}_{-1}^r(\Omega_h)$ as the subspace thereof whose members have vanishing trace along Γ_D .

Remark 7. The conformity requirement $\mathbf{Q}^r(\Omega_h) \subset H^1(\Omega)$ is typically enforced by imposing additional interpolatory constraints on degrees of freedom associated with hanging nodes (*hanging-node constraints*); see [15] for a detailed discussion.

The space $\mathbf{Q}_{-1}^r(\Omega_h)$ can be embedded into the space of distributions over the test space $H^1(\Omega, \Gamma_D)$, i.e., $\mathbf{Q}_{-1}^r(\Omega_h) \subseteq L^2(\Omega) \subseteq H^{-1}(\Omega, \Gamma_N)$. More generally, every $\mathbf{Q}^r(F)$ for $F \in \mathcal{F}_h^I$ with $F \not\subseteq \Gamma_N$ can be identified with a distribution over $H^1(\Omega, \Gamma_D)$ by taking the trace onto F and integrating. Hence we define

$$\mathbf{Q}_{-2}^r(\Omega_h, \Gamma_N) := \mathbf{Q}_{-1}^r(\Omega_h) + \sum_{\substack{F \in \mathcal{F}_h^I \\ F \not\subseteq \Gamma_N}} \mathbf{Q}^r(F),$$

which is a distributional finite element subspace of $H^{-1}(\Omega, \Gamma_N)$.

We also consider finite element spaces of vector fields. We let $\mathbf{RT}^r(K)$ be the Raviart-Thomas space over the full-dimensional cell $K \in \mathbf{Q}_h$, which is formally defined as

$$\mathbf{RT}^r(K) := \bigoplus_{i=1}^n (\mathbf{Q}^r(K) + x_i \mathbf{Q}^r(K)).$$

In other words, the components of each member of $\mathbf{RT}^r(K)$ are polynomials of degree at most r in each coordinate variable except for the i -th variable, which has at most degree $r+1$.

Successively, we introduce the broken Raviart-Thomas space $\mathbf{RT}_{-1}^r(\Omega_h)$ of degree r with respect to the partition Ω_h , (see also [6]), which is

$$\mathbf{RT}_{-1}^r(\Omega_h) := \sum_{K \in \Omega_h} \mathbf{RT}_{-1}^r(K).$$

We define $\mathbf{RT}^r(\Omega_h, \Gamma_N) := \mathbf{H}(\Omega, \Gamma_N, \text{div}) \cap \mathbf{RT}_{-1}^r(\Omega_h)$. We obviously have a well-defined divergence operator

$$\text{div} : \mathbf{RT}^r(\Omega_h, \Gamma_N) \rightarrow \mathbf{Q}_{-1}^r(\Omega_h).$$

More generally, we introduce the piecewise divergence operator

$$\text{div}_h : \mathbf{RT}_{-1}^r(\Omega_h) \rightarrow \mathbf{Q}_{-1}^r(\Omega_h).$$

In addition to that, we consider the jump term operator

$$[\cdot]_{\Omega_h, \Gamma_N} : \mathbf{RT}_{-1}^r(\Omega_h) \rightarrow \sum_{\substack{F \in \mathcal{F}_h^I \\ F \not\subseteq \Gamma_N}} \mathbf{Q}^r(F).$$

Finally, the divergence operator on the broken Raviart-Thomas space is reintroduced in the sense of distributions:

$$\text{div}_{\Omega, \Gamma_N} : \mathbf{RT}_{-1}^r(\Omega_h) \rightarrow \mathbf{Q}_{-2}^r(\Omega_h, \Gamma_N), \quad \tau_h \mapsto \text{div}_h \tau_h - [\tau_h]_{\Omega_h, \Gamma_N}.$$

A fundamental observation, which will be proven shortly, is that for every $s_h \in \mathbf{Q}_{-2}^r(\Omega_h, \Gamma_N)$ there exists $\varrho_h \in \mathbf{RT}_{-1}^r(\Omega_h)$ that solves the flux equation

$$-\text{div}_{\Omega, \Gamma_N} \varrho_h = s_h - \mathcal{H}_{\Omega, \Gamma_D} s_h.$$

This shows the purpose of our definition of $\mathbf{Q}_{-2}^r(\Omega_h, \Gamma_N)$ as giving the right target space for the distributional divergence on the broken Raviart-Thomas space. Let us now prove this existence result.

Lemma 1. *Let $s_h \in \mathbf{Q}_{-2}^r(\Omega_h, \Gamma_N)$. Then there exists $\varrho_h \in \mathbf{RT}_{-1}^r(\Omega_h)$ such that*

$$-\operatorname{div}_{\Omega, \Gamma_N} \varrho_h = s_h - \mathcal{H}_{\Omega, \Gamma_D} s_h.$$

Proof. We fix $s_h \in \mathbf{Q}_{-2}^r(\Omega_h, \Gamma_N)$, which by definition can be written in the form

$$s_h = \sum_{K \in \Omega_h} f_K + \sum_{F \in \mathcal{F}_h^I} j_F,$$

where $f_K \in \mathbf{Q}^r(K)$ for each $K \in \Omega_h$ and $j_F \in \mathbf{Q}^r(F)$ for each $F \in \mathcal{F}_h^I$.

We first note that there exists $\varrho'_h \in \mathbf{RT}_{-1}^r(\Omega_h)$ such that

$$-[\varrho'_h]_{\Omega_h, \Gamma_N} = \sum_{F \in \mathcal{F}_h^I} j_F.$$

We set $s'_h := s_h + \operatorname{div}_{\Omega, \Gamma_N} \varrho'_h = s_h + \operatorname{div}_h \varrho'_h$. By construction, $s'_h \in \mathbf{Q}_{-1}^r(\Omega_h)$, and s'_h annihilates $\mathcal{H}(\Omega, \Gamma_D)$ if and only if s_h annihilates $\mathcal{H}(\Omega, \Gamma_D)$. It remains to construct $\tau_h \in \mathbf{RT}^r(\Omega_h, \Gamma_N)$ such that $\operatorname{div}_{\Omega, \Gamma_N} \tau_h = s'_h$ because then the desired vector field $\varrho_h \in \mathbf{RT}_{-1}^r(\Omega)$ is given by

$$\varrho_h := \varrho'_h + \tau_h.$$

For this purpose we introduce the canonical interpolators

$$\mathbf{I}[\mathbf{RT}^r(\Omega)] : C^\infty(\Omega)^n \rightarrow \mathbf{RT}^r(\Omega),$$

$$\mathbf{I}[\mathbf{Q}^r(\Omega)] : C^\infty(\Omega) \rightarrow \mathbf{Q}^r(\Omega).$$

The former interpolator is defined by

$$\int_K \mathbf{I}[\mathbf{RT}^r(\Omega)] \tau \cdot \phi_K = \int_K \tau \cdot \phi_K, \quad \phi_K \in \bigoplus_{i=1}^n \partial_i \mathbf{Q}^r(K),$$

for all $K \in \Omega_h$ and by

$$\int_F \operatorname{tr}_F \mathbf{I}[\mathbf{RT}^r(\Omega)] \tau \cdot \xi_K = \int_F \operatorname{tr}_F \tau \cdot \xi_K, \quad \xi_K \in \mathbf{Q}^r(F)$$

for $F \in \mathcal{F}_h^I$. The latter interpolator is defined by

$$\int_K \mathbf{I}[\mathbf{Q}^r(\Omega)] f \cdot g_K = \int_K f \cdot g_K, \quad K \in \Omega_h, \quad g_K \in \mathbf{Q}^r(K)$$

for $f \in C^\infty(\Omega)$. Indeed, it follows from the discussion in Section 5 of [6] that this defines members of the finite element spaces $\mathbf{RT}^r(\Omega_h)$ and $\mathbf{Q}_{-1}^r(\Omega_h)$, respectively.

For every $\tau \in C^\infty(\Omega)^n$, $K \in \Omega_h$, and $g_K \in \mathbf{Q}^r(K)$ we find

$$\begin{aligned} \int_K \mathbf{I}[\mathbf{Q}^r(\Omega)] \operatorname{div} \tau \cdot g_K &= \int_K \operatorname{div} \tau \cdot g_K \\ &= \int_K \tau \cdot \nabla g_K + \int_{\partial K} \operatorname{tr}_N \tau \cdot \operatorname{tr} g_K \\ &= \int_K \mathbf{I}[\mathbf{RT}^r(\Omega)] \tau \cdot \nabla g_K + \int_{\partial K} \operatorname{tr}_N \tau \cdot \operatorname{tr} g_K. \end{aligned}$$

The boundary integral is given as a combination of face integrals over K . On a uniform mesh, we could now replace the face integrals of τ by the face integrals of $\mathbf{I}[\mathbf{RT}^r(\Omega)] \tau$ and revert the integration by parts. But since we allow meshes with hanging nodes, it may happen that the faces of K do not represent degrees of freedom over $\mathbf{RT}^r(\Omega)$. The trick is that a repeated application of the integration

by parts formula allows us to express the integral as a combination of degrees of freedom of τ associated to further full-dimensional quadrilaterals and associated to faces in \mathcal{F}_h^I . We can then replace these by degrees of freedom of $\mathbf{I}[\mathbf{RT}^r(\Omega)]\tau$ and apply the integration by parts formulas in the reverse order to obtain that

$$\int_K \mathbf{I}[\mathbf{Q}^r(\Omega)] \operatorname{div} \tau \cdot g_K = \int_K \operatorname{div} \mathbf{I}[\mathbf{RT}^r(\Omega)] \tau \cdot g_K.$$

This eventually implies that

$$\operatorname{div} \mathbf{I}[\mathbf{RT}^r(\Omega)] \tau = \mathbf{I}[\mathbf{Q}^r(\Omega)] \operatorname{div} \tau.$$

So the canonical interpolants commute with the exterior derivative.

Since functions in $\mathbf{H}(\Omega, \operatorname{div})$ have well-defined traces on the codimension one faces of Ω_h with regularity $\mathbf{H}^{-\frac{1}{2}}$, we conclude that we have bounded operators

$$\begin{aligned} \mathbf{I}[\mathbf{RT}^r(\Omega)] : \mathbf{H}(\Omega, \operatorname{div}) &\rightarrow \mathbf{RT}^r(\Omega) \subset \mathbf{L}^2(\Omega), \\ \mathbf{I}[\mathbf{Q}^r(\Omega)] : L^2(\Omega) &\rightarrow \mathbf{Q}^r(\Omega) \subset L^2(\Omega). \end{aligned}$$

Moreover, when $\tau \in \mathbf{H}(\Omega, \operatorname{div})$ has vanishing normal trace on the faces of Γ_N , then the same holds true for its canonical interpolation $\mathbf{I}[\mathbf{RT}^r(\Omega)](\tau)$. In particular, we have a bounded operator

$$\mathbf{I}[\mathbf{RT}^r(\Omega)] : \mathbf{H}(\Omega, \operatorname{div}, \Gamma_N) \rightarrow \mathbf{RT}^r(\Omega_h, \Gamma_N) \subset \mathbf{L}^2(\Omega).$$

These observations are applied as follows. There exists $\tau \in \mathbf{H}(\Omega, \operatorname{div}, \Gamma_N)$ such that $\operatorname{div} \tau = s'_h$, as follows from the Poincaré-Friedrichs inequality (6) and the fact that $s'_h \in L^2(\Omega)$ annihilates $\mathcal{H}(\Omega, \Gamma_D)$. We set $\tau_h = \mathbf{I}[\mathbf{RT}^r(\Omega)]\tau$ and see

$$\begin{aligned} \operatorname{div} \tau_h &= \operatorname{div} \mathbf{I}[\mathbf{RT}^r(\Omega)]\tau \\ &= \mathbf{I}[\mathbf{Q}^r(\Omega)] \operatorname{div} \tau = \mathbf{I}[\mathbf{Q}^r(\Omega)] s'_h = s'_h. \end{aligned}$$

This completes the proof. \square

4.2. Localized Flux Reconstruction. After this preparation, we approach the solution of the residual flux equation. Given a distributional finite element right-hand side $F_h \in \mathbf{Q}_{-2}^r(\Omega_h, \Gamma_N)$, we let $u_h \in \mathbf{Q}^{r+1}(\Omega_h, \Gamma_D)$ be the unique solution of

$$\int_{\Omega} \nabla u_h \cdot A \nabla v_h = F_h(v_h - \mathcal{H}_{\Omega, \Gamma_D} v_h), \quad v_h \in \mathbf{Q}^{r+1}(\Omega_h, \Gamma_D).$$

In order to facilitate the equilibrated error estimator we seek a solution $\sigma_h \in \mathbf{RT}_{-1}^r(\Omega_h)$ to the finite element flux equation

$$(22) \quad -\operatorname{div}_{\Omega, \Gamma_N} A \sigma_h = F_h - \mathcal{H}_{\Omega, \Gamma_D} F_h.$$

Note that (22) is well-posed according to Lemma 1. Hence, this equation can be solved in the sense of least-squares with respect to the A -norm. Moreover, if $F_h \in \mathbf{Q}_{-1}^r(\Omega)$ is a square-integrable function, then the variable σ_h may be sought in $\mathbf{RT}^r(\Omega_h, \Gamma_N)$. In this sense (22), the finite element flux equation can be solved with computational costs comparable to a mixed finite element method. In particular, the approximate solution u_h does not enter the construction.

However, the Galerkin approximation u_h contains additional information that facilitates a localized solution of the flux equation. The solution constructed in that manner will generally not minimize the A -norm, though.

To begin with, we define the residual $r_h \in \mathbf{Q}_{-2}^r(\Omega_h, \Gamma_N) \subseteq H^{-1}(\Omega, \Gamma_N)$ by

$$r_h := (\text{Id} - \mathcal{H}_{\Omega, \Gamma_D}) F_h + \text{div}_{\Omega, \Gamma_N} A \nabla u_h.$$

Our goal is to construct a vector field $\varrho_h \in \mathbf{RT}_{-1}^r(\Omega_h)$ solving the finite element residual flux equation

$$(23) \quad -\text{div}_{\Omega, \Gamma_N} A \varrho_h = r_h.$$

Again, this system has a proper solution, which in theory can be directly constructed from the any solution of (22). For the implementation of the localized flux reconstruction, though, we construct a solution of (22) with the help of a solution of (23).

In order to discuss this, we introduce a partition of unity. For every non-hanging node $v \in \mathcal{N}_h^I$ we let $\psi^V \in \mathbf{Q}^1(\Omega_h)$ be defined by requiring that ψ^V takes the value 1 at the node $v \in \mathcal{N}_h^I$ and the value 0 at all other non-hanging nodes in \mathcal{N}_h^I . The support $\omega^V := \text{supp } \psi^V$ is a subdomain of Ω . It is evident that the collection of all such ψ^V constitutes a partition of unity over Ω .

We let ω_h^V be the *patch* of elements around v , which forms a partition of ω^V . In addition, we define the local boundary patches

$$\gamma_D^V := \begin{cases} \partial\omega^V \cap \Gamma_D & \text{if } V \in \Gamma_D, \\ \emptyset & \text{if } V \notin \Gamma_D, \end{cases} \quad \gamma_N^V := \partial\omega^V \setminus \overline{\gamma_D^V}.$$

It is important to note that every local patch ω^V is a contractible Lipschitz domain. In particular, $\mathcal{H}(\omega^V, \gamma_D^V)$ is either zero or spanned by the constant functions over the patch ω^V depending on whether γ_D^V is non-empty or not.

For every $v \in \mathcal{N}_h^I$ being a non-hanging node, we define the localized residual as the distribution $r_h^V := \psi^V r_h$. Note that $r_h^V \in \mathbf{Q}_{-2}^{r+1}(\omega_h^V, \gamma_N^V)$. Moreover, for any function $1_V \in \mathcal{H}_D(\omega^V, \gamma_D^V)$ with constant value 1 we have

$$r_h^V(1_V) = r_h^V(\psi_h^V) = 0.$$

This follows by the definition of the residual together with Galerkin orthogonality.

Consequently, Lemma 1 gives the existence of a solution $\varrho_h^V \in \mathbf{RT}_{-1}^{r+1}(\omega^V)$ to the localized problem

$$-\text{div}_{\Omega, \Gamma_N} \varrho_h^V = r_h^V.$$

Definitions show that the sum

$$(24) \quad \varrho_h^L := \sum_{v \in \mathcal{N}_h^I} \varrho_h^V$$

is a solution to the residual flux equation (23). A solution to the finite element flux equation is then given by

$$\sigma_h^L := \varrho_h + \nabla u_h \in \mathbf{RT}^{r+1}(\Omega_h, \Gamma_N).$$

4.3. Applications. We assume that $F \in H^{-1}(\Omega, \Gamma_N)$ and that $u \in H^1(\Omega, \Gamma_D)$ is the unique solution of

$$(25) \quad -\text{div}_{\Omega, \Gamma_N} A \nabla u = F - \mathcal{H}_{\Omega, \Gamma_D} F, \quad u \perp \mathcal{H}(\Omega, \Gamma_D).$$

Under the special assumption that $F \in \mathbf{Q}^r(\Omega_h, \Gamma_N)$ we can immediately instantiate the flux reconstruction (either global or localized) to obtain

$$\|\nabla u - \nabla u_h\|_A \leq \|\nabla u_h - \sigma_h\|_A.$$

In general, we cannot assume that F is a member of $\mathbf{Q}_{-2}^r(\Omega_h, \Gamma_N)$. Hence the flux reconstruction is performed by solving an approximate flux equation with an approximate right-hand side $F_h \in \mathbf{Q}_{-2}^r(\Omega, \Gamma_N)$. Given any discrete flux $\sigma_h \in \mathbf{RT}^{r+1}(\Omega_h, \Gamma_N)$ solving

$$(26) \quad -\operatorname{div}_{\Omega, \Gamma_N} A \sigma_h = F_h - \mathcal{H}_{\Omega, \Gamma_D} F_h,$$

we can utilize the generalized error estimates of the previous section.

The discrete flux $\sigma_h \in \mathbf{RT}^{r+1}(\Omega_h, \Gamma_N)$ can of course be obtained by solving a global finite element system. Let $\sigma_h^G \in \mathbf{RT}^{r+1}(\Omega_h, \Gamma_N)$ denote this flux reconstruction, which is obtained by solving (26) with minimal A -norm over Ω . We also write $\varrho_h^G := \sigma_h^G - \nabla u_h \in \mathbf{RT}_{-1}^{r+1}(\Omega_h)$ for the corresponding solution of the residual flux equation.

The localization of the flux reconstruction with approximate data requires additional assumptions. The reason is that the localized flux reconstruction requires a local equilibration condition; since u_h satisfies the Galerkin condition with respect to F but generally not with respect to F_h , it is not immediately clear how the localized construction can be generalized.

As a solution we impose an additional condition: we require that

$$(27) \quad (F - F_h)(v_h) = 0, \quad v_h \in \mathbf{Q}^1(\Omega_h, \Gamma_D).$$

Under that condition we have

$$F_h(\psi^V) - \langle \nabla u_h, \nabla \psi^V \rangle_A = F(\psi^V) - \langle \nabla u_h, \nabla \psi^V \rangle_A$$

for all non-hanging nodes $V \in \mathcal{N}_h^I$ with $V \notin \Gamma_D$. Consequently, the local problems in the localized flux reconstruction are well-posed, and thus a solution $\varrho_h \in \mathbf{RT}_{-1}^{r+1}(\Omega_h)$ to the *approximate residual flux equation*

$$-\operatorname{div}_{\Omega, \Gamma_N} A \varrho_h = (\operatorname{Id} - \mathcal{H}_{\Omega, \Gamma_D}) F_h + \operatorname{div} A \nabla u_h$$

is found by adding the local solutions. As before, a solution to (26) is now given by $\sigma_h := \varrho_h - \nabla u_h$. A reliable error estimates (even in the case $F \neq F_h$) is then given via (18). To quantify the efficiency of this error estimate we may use (19).

Finally, for our study of adaptive finite element methods later in this article we introduce the local error indicators

$$(28) \quad \eta_K(\varrho_h) := \|\varrho_h\|_{\mathbf{L}_A^2(K)}^2.$$

4.4. Improved Estimates. The aforementioned error estimates and efficiency estimates are of very general nature. The additional structure given by the finite element setting enables some interesting further results that quantify the influence of the error $F - F_h$ in the data. These techniques, however, utilize additional regularity assumptions:

$$(29) \quad F, F_h \in L^2(\Omega),$$

$$(30) \quad F - F_h \perp \mathbf{Q}_{-1}^0(\Omega_h).$$

We begin with a lower bound for the error estimator. It is a basic fact that

$$\|\nabla u - \nabla u_h\|_A = \sup_{\substack{w \in H^1(\Omega, \Gamma_D), \\ w \perp \mathcal{H}(\Omega, \Gamma_D)}} \frac{\langle \nabla u - \nabla u_h, \nabla w \rangle_A}{\|\nabla w\|_A}.$$

Let \widehat{u} be the solution of the Poisson equation analogous to (25) but with the data F being replaced by the approximate data F_h . If $\varrho_h \in \mathbf{RT}_{-1}^{r+1}(\Omega_h)$ solves (26), then we can use

$$\begin{aligned} \langle \nabla u - \nabla u_h, \nabla w \rangle_A &= \langle \nabla u - \nabla \widehat{u}, \nabla w \rangle_A + \langle \nabla \widehat{u} - \nabla u_h, \nabla w \rangle_A \\ &= \langle F - F_h, w \rangle + \langle \nabla \widehat{u} - \nabla u_h, \nabla w \rangle_A \\ &= \langle F - F_h, w \rangle + \langle \varrho_h, \nabla w \rangle_A \\ &= \langle F - F_h, w - w_h \rangle + \langle \varrho_h, \nabla w \rangle_A, \end{aligned}$$

where in the last step $w_h \in \mathbf{Q}^1(\Omega, \Gamma_D)$ can be chosen arbitrarily due to condition (27). By picking w_h as the first-order Clément interpolant of w (see [15] for a discussion) one now sees that

$$(31) \quad \|\nabla u - \nabla u_h\|_A \leq \|\varrho_h\|_A + C_I \sum_{K \in \Omega_h} h_K \|F - F_h\|_{L^2(K)},$$

where the constant $C_I > 0$ depends only on C_h .

On the other hand, we prove a converse upper bound for the error estimator specifically for the residual flux reconstruction ϱ_h^L . We have

$$\|\varrho_h^L\|_{\mathbf{L}_A^2(K)} \leq \sum_{V \in \mathcal{N}_h^I(K)} \|\varrho_h^V\|_{\mathbf{L}_A^2(K)} \leq \sum_{V \in \mathcal{N}_h^I(K)} \|\varrho_h^V\|_{\mathbf{L}_A^2(\omega^V)}.$$

A scaling argument with a constant $C > 0$ depending only on the mesh-constant and the polynomial degree yields that

$$\|\varrho_h^V\|_{\mathbf{L}_A^2(\omega^V)} \leq C \|\nabla u - \nabla u_h\|_{\mathbf{L}_A^2(\omega^V)} + C \sum_{K \in \omega_h^V} h_K \|F_h - F\|_{L^2(K)}.$$

Finally, we address the relation between the flux reconstructions σ_h^L , the minimum norm solution σ_h^G over $\mathbf{RT}^{r+1}(\Omega_h, \Gamma_N)$, and the true flux ∇u . Since the flux reconstruction σ_h^L can be obtained just as much from the distributional divergence of the flux reconstruction σ_h^G , a scaling argument easily gives

$$(32) \quad \|\varrho_h^L\|_{\mathbf{L}_A^2(K)} + \|\varrho_h^G - \varrho_h^L\|_{\mathbf{L}_A^2(K)} \leq C \sum_{V \in \mathcal{N}_h^I(K)} \|\varrho_h^G\|_{\mathbf{L}_A^2(\omega^V)}.$$

We conclude that the local flux reconstruction will typically not be much worse than the global flux reconstruction in numerical tests. Note that the generic constant $C > 0$ in (32), which depends only the mesh constant and the polynomial, satisfies a computable bound.

The global flux reconstruction is equivalent to the solution of a mixed finite element method. In typical applications ∇u and $\nabla \widehat{u}$ are contained in a higher order Sobolev space such as $\mathbf{H}^s(\Omega)$ for a parameter $s \in [0.5, 1]$ that depends only on the domain. Consequently, we have

$$\begin{aligned} \|\sigma_h^G - \nabla u\|_A &\leq \|\nabla \widehat{u} - \nabla u\|_A + \|\sigma_h^G - \nabla \widehat{u}\|_A \\ &\leq C \sum_{K \in \Omega_h} \left(h_K \|F_h - F\|_A + h_K^s \|\nabla \widehat{u}\|_{\mathbf{H}^s(K)} \right). \end{aligned}$$

Hence the differences

$$\theta_h^G := \sigma_h^G - \nabla \widehat{u}, \quad \theta_h^L := \sigma_h^L - \nabla \widehat{u},$$

which are members of $\mathbf{X}(\Omega, \Gamma_N, A)$ as defined in (7), are controlled by terms of higher order. The two vector fields θ_h^G and θ_h^L measure how far the respective flux reconstructions differ from the true gradients.

Remark 8. Our analysis of the influence of $F - F_h$ on the overall data is inspired by earlier discussions in the literature, in particular the work of Braess and Schöberl [12]. Their construction of the local problems in the case $F \neq F_h$ is different from ours though (see [10]).

Remark 9. The label *equilibrated error estimator* is motivated by the localized solution of the flux equation based on local Neumann problems whose right-hand sides satisfy the equilibrium condition, i.e., annihilate the constant functions. In this article we treat error estimators based on solving local Poisson problems in mixed formulations. The term *equilibrated error estimator*, however, is shared with another family of error estimators that solve local Poisson problems in elliptic formulation over either local patches or single elements (see [19, 7, 2, 24, 1]). Even though there exists extensive literature on the latter type of error estimators for a variety of different finite element spaces, it seems that much less has been published for the former family of equilibrated error estimators.

Equilibrated error estimators are often contrasted to the classical residual error estimator: then the latter is called *explicit* because it derives estimates directly from bounding the negative norm of the residual, which involves mesh-dependent norms on the volume and face terms of the residual. Equilibrated residual error estimators, on the other hand, are called *implicit* because they bound the negative norm of the residual in terms of a flux reconstruction associated with the residual.

5. ERROR ESTIMATION FOR QUANTITIES OF INTEREST

In many applications we are primarily interested in determining a specific *quantity of interest*. For the sake of simplicity, we assume these to be linear functionals of the solution. Goal-oriented a posteriori error estimation aims at sharp error estimates in and adaptivity optimized towards the approximation of the quantity of interest. All but the most simplistic approaches towards goal-oriented a posteriori error estimation require the computation of Galerkin solutions of both the original primal and a dual problem of the same kind. In this section we review some techniques proposed in the literature [8, 25, 18] and suggest a new heuristic approximation for the error in the quantity of interest.

5.1. Basic Theory. We reconsider the Poisson problem from Section 3, where $A \in L^\infty(\Omega)^{n \times n}$ is an admissible metric tensor and $F \in H^{-1}(\Omega, \Gamma_N)$ is the right-hand side. Additionally, we let $J \in H^{-1}(\Omega, \Gamma_N)$ be a functional. We are interested in the value $J(u)$, where $u \in H^1(\Omega, \Gamma_D)$ solves the following Poisson problem:

$$(33) \quad -\operatorname{div}_{\Omega, \Gamma_N} A \nabla u = F - \mathcal{H}_{\Omega, \Gamma_D} F, \quad u \perp \mathcal{H}(\Omega, \Gamma_D).$$

The functional J is also called *goal functional* in the literature. Now suppose that $u_h \in H^1(\Omega, \Gamma_D)$ is any computable approximation of u . We are interested in estimating the error $J(u) - J(u_h)$ in the goal functional without using the generally unknown true solution of the Poisson problem.

A central concept in the error estimation of linear functionals is the *dual problem*. This constitutes in determining the *dual quantity of interest* $F(z)$, where

$z \in H^1(\Omega, \Gamma_D)$ solves the Poisson problem

$$(34) \quad -\operatorname{div}_{\Omega, \Gamma_N} A \nabla z = J - \mathcal{H}_{\Omega, \Gamma_D} J, \quad z \perp \mathcal{H}(\Omega, \Gamma_D).$$

Accordingly, we call the problem of determining the *primal quantity of interest* $J(u)$ the *primal problem*. The well-posedness of (33) and (34) is clear by our discussion in Section 2. F is the *primal right-hand side* and the *dual goal functional*, while J is the *dual right-hand side* and the *primal goal functional*. We call u and z the *primal solution* and the *dual solution*, respectively. The elementary identity

$$(35) \quad J(u) = \langle \nabla u, \nabla z \rangle_A = F(z)$$

states that the primal and the dual quantities of interest coincide.

In the sequel we apply this idea to finite element approximations. We fix a cubical partition Ω_h of the domain Ω such that a subset of the faces is a partition of Γ_D . Moreover we let $r \in \mathbb{N}$ be a fixed non-negative integer that denotes the polynomial degree. We assume to be given both an approximation $u_h \in H^1(\Omega, \Gamma_D)$ of the primal solution and an approximation $z_h \in H^1(\Omega, \Gamma_D)$ of the dual solution. We specifically require these to be Galerkin solutions in the sense that $u_h, z_h \in \mathbf{Q}^r(\Omega, \Gamma_D)$ satisfy

$$(36a) \quad \langle \nabla u_h, \nabla v_h \rangle_A = F(v_h - \mathcal{H}_{\Omega, \Gamma_D} v_h), \quad v_h \in \mathbf{Q}^r(\Omega, \Gamma_D),$$

$$(36b) \quad \langle \nabla z_h, \nabla v_h \rangle_A = J(v_h - \mathcal{H}_{\Omega, \Gamma_D} v_h), \quad v_h \in \mathbf{Q}^r(\Omega, \Gamma_D).$$

To ensure uniqueness we may enforce the usual orthogonality conditions $u_h \perp \mathcal{H}(\Omega, \Gamma_D)$ and $z_h \perp \mathcal{H}(\Omega, \Gamma_D)$, but this will not be central in the sequel. A simple but important consequence of (36) is Galerkin orthogonality:

$$(37a) \quad \langle \nabla(u - u_h), \nabla v_h \rangle_A = 0, \quad v_h \in \mathbf{Q}^r(\Omega, \Gamma_D),$$

$$(37b) \quad \langle \nabla(z - z_h), \nabla v_h \rangle_A = 0, \quad v_h \in \mathbf{Q}^r(\Omega, \Gamma_D).$$

We call u_h and z_h the *primal* and the *dual Galerkin solution*, respectively. Using definitions and Galerkin orthogonality, we find

$$(38) \quad J(u - u_h) = \langle \nabla u - \nabla u_h, \nabla z - \nabla z_h \rangle_A = F(z - z_h).$$

In other words, the error in the quantity of interest equals the product of the primal and the dual gradient errors. We derive various goal-oriented error estimators by computing an upper bound for the error product $\langle \nabla u - \nabla u_h, \nabla z - \nabla z_h \rangle_A$, which we henceforth call the *error of interest*.

Remark 10. The energy error is a special quantity of interest. If $J = F$ and $u_h = z_h$, then the primal and the dual quantities of interest (35) coincide with the energy norm of the error, and the error of interest (38) is then the energy error of the Galerkin solution.

Remark 11. An additional source of error has not been discussed yet: in applications, the Galerkin solutions are not computed exactly but only up to a certain numerical accuracy. Consequently, a posteriori error estimates must in principle take into account the deviation from Galerkin orthogonality (see [4]). This is not within the scope of this article.

5.2. Review of Flux Reconstruction. We briefly discuss flux reconstructions for the primal and the dual problem and settle some notation. We define the *primal residual* $r_h \in H^{-1}(\Omega, \Gamma_N)$ and the *dual residual* $s_h \in H^{-1}(\Omega, \Gamma_N)$ by

$$(39a) \quad r_h := F - \mathcal{H}_{\Omega, \Gamma_D} F + \operatorname{div}_{\Omega, \Gamma_N} A \nabla u_h,$$

$$(39b) \quad s_h := J - \mathcal{H}_{\Omega, \Gamma_D} J + \operatorname{div}_{\Omega, \Gamma_N} A \nabla z_h.$$

We introduce the residual flux equations

$$(40) \quad -\operatorname{div}_{\Omega, \Gamma_N} A \varrho_h = r_h, \quad -\operatorname{div}_{\Omega, \Gamma_N} A \varpi_h = s_h.$$

The gradient error vector fields of the primal and the dual problem,

$$(41) \quad \varrho_h^{\text{opt}} := \nabla u - \nabla u_h, \quad \varpi_h^{\text{opt}} := \nabla z - \nabla z_h,$$

solve the residual flux equations. They are optimal solutions in the sense that their \mathbf{L}^2 -norm are minimal among the respective solution sets. Hence

$$(42) \quad J(u - u_h) = \langle \varrho_h^{\text{opt}}, \varpi_h^{\text{opt}} \rangle_A = F(z - z_h).$$

This identity expresses the error of interest as the product of the optimal residual flux reconstructions. Of course, this result is practically inaccessible: if the minimum norm residual flux reconstructions ϱ_h^{opt} and ϖ_h^{opt} were known, then we could easily recover the true gradients ∇u and ∇z of the primal and the dual solution.

In many applications, however, it is possible to compute finite element solutions $\varrho_h \in \mathbf{RT}_{-1}^r(\Omega)$ and $\varpi_h \in \mathbf{RT}_{-1}^r(\Omega)$ to the residual flux equations (40) that are close to the optimal solutions ϱ_h^{opt} and ϖ_h^{opt} . We then have the Hodge-Helmholtz decompositions

$$\varrho_h = \varrho_h^{\text{opt}} + \theta_h, \quad \varpi_h = \varpi_h^{\text{opt}} + \zeta_h$$

for uniquely determined $\theta_h, \zeta_h \in \mathbf{X}(\Omega, \Gamma_N, A)$. Accordingly, we find by the A -orthogonality of the Hodge-Helmholtz decomposition that

$$(43) \quad \langle \varrho_h, \varpi_h \rangle_A = \langle \varrho_h^{\text{opt}}, \varpi_h^{\text{opt}} \rangle_A + \langle \theta_h, \zeta_h \rangle_A.$$

Lastly, we recall that the flux reconstructions

$$\sigma_h = \varrho_h + \nabla u_h, \quad \tau_h = \varpi_h + \nabla z_h$$

solve the primal and the dual flux equations

$$(44) \quad -\operatorname{div}_{\Omega, \Gamma_N} A \sigma_h = F - \mathcal{H}_{\Omega, \Gamma_D} F, \quad -\operatorname{div}_{\Omega, \Gamma_N} A \tau_h = J - \mathcal{H}_{\Omega, \Gamma_D} J.$$

5.3. Heuristic Error Computation. We first recall some constant-free reliable error estimates that make use of a (global) Cauchy-Schwarz inequality. The most immediate approach is to trace back the error of interest to the error in the primal problem. Here one uses

$$(45) \quad \begin{aligned} J(u - u_h) &= \langle \nabla u - \nabla u_h, \nabla z \rangle_A \\ &\leq \|\nabla u - \nabla u_h\|_A \cdot \|\nabla z\|_A \leq \|\varrho_h\|_A \cdot \|\tau_h\|_A \end{aligned}$$

A different variant uses the Galerkin orthogonality in the primal problem. We have

$$(46) \quad \begin{aligned} J(u - u_h) &= \langle \nabla u - \nabla u_h, \nabla z - \nabla z_h \rangle_A \\ &\leq \|\nabla u - \nabla u_h\|_A \cdot \|\nabla z - \nabla z_h\|_A \leq \|\varrho_h\|_A \cdot \|\varpi_h\|_A \end{aligned}$$

Both estimates are reliable and constant free. In applications we expect the error estimate $\|\varrho_h\|_A \cdot \|\varpi_h\|_A$ to converge with twice the rate of the error estimate $\|\varrho_h\|_A$.

$\|\tau_h\|_A$, which indicates that error estimates for the primal problem alone lead to suboptimal error estimates.

Remark 12. The error estimates (45) and (46) have been the starting point for several marking strategies in finite element methods. Feischl, Praetorius, and van der Zee [18] have investigated strategies of how to combine the information of local error estimators for the primal and the dual problem in order to drive goal-oriented adaptivity.

The most obvious problem with estimators based on the global Cauchy-Schwarz inequality is the overestimation of the true error since cancellation effects inside the integral $\langle \nabla u, \nabla z \rangle_A$ are not taken into account: if ∇u and ∇z are nearly A -orthogonal to each other, then the overestimation will be substantial.

This has motivated a variety of error estimators that approximate the error $J(u - u_h)$ by a computable integral. Consequently, these techniques give *error approximations* rather than *error estimates*. On the one hand, these techniques are generally heuristic and may suffer from massive underestimation of the error [26]. On the other hand, the incorporation of cancellation effects achieves very accurate approximations for the true error of interest in applications.

We review some computable approximations for the error of interest $J(u - u_h)$. We first see

$$J(u - u_h) = \langle \nabla u - \nabla u_h, \nabla z \rangle_A = \langle \sigma_h - \nabla u_h, \nabla \tau_h \rangle_A - \langle \theta_h, \zeta_h \rangle_A.$$

Neglecting the term $\langle \theta_h, \zeta_h \rangle_A$, which is generally not computable we come to the error approximation

$$(47) \quad J(u - u_h) \approx \eta^{\sigma\tau} := \langle \sigma_h - \nabla u_h, \tau_h \rangle_A = \langle \varrho_h, \tau_h \rangle_A$$

and the local error indicators

$$(48) \quad \eta_K^{\sigma\tau} := \int_K \varrho_h \cdot A\tau_h \, dx, \quad K \in \Omega_h.$$

It is intuitive that this error estimate can be improved by using the Galerkin orthogonality of the primal problem. We have

$$\begin{aligned} J(u - u_h) &= \langle \nabla u - \nabla u_h, \nabla z - \nabla z_h \rangle_A \\ &= \langle \sigma_h - \nabla u_h, \tau_h - \nabla z_h \rangle_A - \langle \theta_h, \zeta_h \rangle_A \\ &= \langle \varrho_h, \varpi_h \rangle_A - \langle \theta_h, \zeta_h \rangle_A. \end{aligned}$$

Again neglecting the term $\langle \theta_h, \zeta_h \rangle_A$, we consider the approximation

$$(49) \quad J(u - u_h) \approx \eta^{\sigma\varpi} := \langle \varrho_h, \varpi_h \rangle_A.$$

The corresponding local error indicators are

$$(50) \quad \eta_K^{\sigma\varpi} := \int_K \varrho_h \cdot A\varpi_h \, dx, \quad K \in \Omega_h.$$

Remark 13. The error approximations (47) and (49) are, of course, the same, but we state these different formulas because they inspire the different local error indicators (48) and (50), respectively. In fact, the error indicators (48) have been proposed by Mozolevski and Prudhomme [25], who have investigated goal-oriented equilibrated error estimation for a variety of discontinuous Galerkin finite element methods. They focus, however, on the special case of full elliptic regularity, where

they numerically observed optimal adaptive convergence. Curiously, the local indicators (50) have apparently not been investigated before in the literature.

The size of the error term $\langle \theta, \zeta \rangle_A = \langle \sigma_h - \nabla u_h, \tau_h - \nabla z \rangle_A$ is decisive for the approximation quality of η^{err} and η^{err} . When the flux reconstructions σ_h and τ_h are obtained by a mixed finite element method, then the product $\langle \theta, \zeta \rangle_A$ can be controlled by convergence estimates for the mixed finite element method. Due to Inequality (32), this is only slightly worse by a generic constant when the localized flux reconstruction is used instead. Since the polynomial degree (or the local mesh resolution) in the localized flux reconstruction can be increased with only constant factor in the computational effort, we expect the error product $\langle \theta, \zeta \rangle_A$ to be negligible in applications where ∇u and ∇z feature sufficiently high regularity. This gives reasonable hope that η^{err} and η^{err} approximate the true error in many applications.

The preceding local indicators are based on the approximation $\nabla z \approx \tau_h$, which holds true up to $\mathbf{X}(\Omega, \Gamma_N, A)$, i.e., the error of this approximation is orthogonal to gradients. Another possibility is to approximate ∇z by the gradient ∇z_h^* of an approximation z_h^* of the dual solution z , i.e., $\nabla z \approx \nabla z_h^*$. Due to Galerkin orthogonality we should not choose any $z_h^* \in \mathbf{Q}^r(\Omega_h, \Gamma_D)$ since that would give a useless trivial approximation. A practically relevant method is constructing z_h^* from z_h in a higher order space on a coarser mesh (see [9]).

With this background in mind, we observe that

$$\begin{aligned} J(u - u_h) &= \langle \nabla u - \nabla u_h, \nabla z \rangle_A \\ &= \langle \nabla u - \nabla u_h, \nabla z_h^* \rangle_A - \langle \nabla u - \nabla u_h, \nabla z_h^* - \nabla z \rangle_A \\ &= \langle \sigma_h - \nabla u_h, \nabla z_h^* \rangle_A - \langle \nabla u - \nabla u_h, \nabla z_h^* - \nabla z \rangle_A \end{aligned}$$

If we assume that the product $\langle \nabla u - \nabla u_h, \nabla z_h^* - \nabla z \rangle_A$ is negligible, then this suggests the error approximation

$$(51) \quad J(u - u_h) \approx \eta^{\text{I},*} := \langle \sigma_h - \nabla u_h, \nabla z_h^* \rangle_A$$

and the corresponding error indicators

$$(52) \quad \eta_K^{\text{I},*} := \int_K \varrho_h \cdot A \nabla z_h^* \, dx, \quad K \in \Omega_h.$$

Again, the primal Galerkin orthogonality can be used for what promises to be an improvement. We then easily find in a manner similar as above that

$$J(u - u_h) = \langle \sigma_h - \nabla u_h, \nabla z_h^* - \nabla z_h \rangle_A - \langle \nabla u - \nabla u_h, \nabla z_h^* - \nabla z \rangle_A.$$

A promising error approximation is given by

$$(53) \quad J(u - u_h) \approx \eta^{\text{II},*} := \langle \sigma_h - \nabla u_h, \nabla z_h^* - \nabla z_h \rangle_A$$

with associated local error indicators

$$(54) \quad \eta_K^{\text{II},*} := \int_K \varrho_h \cdot A (\nabla z_h^* - \nabla z_h) \, dx, \quad K \in \Omega_h.$$

Remark 14. The error approximations $\eta^{\text{I},*}$ and $\eta^{\text{II},*}$ and the associated error indicators $\eta_K^{\text{I},*}$ and $\eta_K^{\text{II},*}$ are inspired by dual weighted residual methods [8]. As a motivation for this class of goal-oriented error estimations we first assume for the sake of simplicity that A is piecewise constant and $F \in L^2(\Omega)$. We then observe that

$$\langle \nabla u - \nabla u_h, \nabla z_h^* - \nabla z_h \rangle_A$$

$$= \sum_{K \in \Omega_h} \int_K F(z_h^* - z_h) \, dx - \oint_{\partial K} \text{tr}_{\partial K}(z_h^* - z_h) \cdot \text{tr}_{N,K} A \nabla u_h \, ds.$$

This has motivated the error approximation $\eta^{\text{DWR},*}$ and the local error indicators $\eta_K^{\text{DWR},*}$ of the dual weighted residual method, defined by

$$(55) \quad \eta^{\text{DWR},*} := \sum_{K \in \Omega_h} \eta_K^{\text{DWR},*}$$

$$(56) \quad \eta_K^{\text{DWR},*} := \int_K F(z_h^* - z_h) \, dx - \oint_{\partial K} \text{tr}_{\partial K}(z_h^* - z_h) \cdot \text{tr}_{N,K} A \nabla u_h \, ds.$$

Our error indicators $\eta_K^{\text{II},*}$ mimic the construction of the dual weighted residual error indicators $\eta_K^{\text{DWR},*}$ but are not identical to them. The error approximations $\eta^{\text{DWR},*}$ and $\eta^{\text{II},*}$, however, are identical.

Due to Galerkin orthogonality, the dual finite element approximation z_h can be removed from the definition of $\eta^{\text{DWR},*}$ without changing the value; it makes a difference, however, whether the term z_h appears in the local error indicators $\eta_K^{\text{DWR},*}$ or not. It has long been known that the omission of z_h will generally lead to suboptimal adaptive marking strategies. This is analogous to our earlier observation regarding the global Cauchy-Schwarz inequality. In practice, we expect the indicators $\eta_K^{\text{I},*}$ to perform similar to $\eta^{\text{I},*}$ and notably worse than $\eta^{\text{II},*}$.

Remark 15. There are several liberties in the exact definition of the local error indicators but typically these have little effect on the overall performance in practice. We have stated the error indicators as cellwise integrals as recommended by Becker and Rannacher (see Equation (3.19) of [8]) for the dual weighted residual method, but it is also common to apply an additional Cauchy-Schwarz inequality to the local integrals (see Equation (3.18) in the same reference). Furthermore, the dual Galerkin approximation z_h in the definition of our error indicators can in practice be replaced by any other “reasonable” approximation of z in the finite element space $\mathbf{Q}^r(\Omega, \Gamma_D)$. Lastly, regarding specifically the error indicators $\eta_K^{\text{II},*}$ and their relatives, we mention that there are many possible ways to pick an approximation z_h^* , see also Section 5 of [8]. We utilize a higher order interpolation on a coarser mesh for our computational experiments in the next section.

6. NUMERICAL EXPERIMENTS

In this section we present a number of numerical experiments that document properties of our proposed local patch-wise flux reconstruction, the global equilibrated error estimator, and our heuristic goal-oriented error estimators. All numerical experiments have been computed with the help of the finite element library Deal.II [5]. Solutions of linear problems (on global meshes and local patches) have been computed with a direct solver [17].

First, we demonstrate the efficiency of equilibrated error estimators when the flux reconstruction is conducted locally (as discussed in Section 4) or globally (akin to mixed finite element methods). We successively document optimal convergence of an adaptive finite element method driven by equilibrated error estimators. Furthermore, we assess the performance of the error approximations and indicators proposed in Section 5; our numerical experiments document the efficiency under global uniform refinement and as drivers in goal-oriented adaptive finite element methods.

6.1. Test Cases. Our numerical experiments have been carried out for two prototypical test cases. We consider the model Poisson equation (9) over two different domains: the unit square Ω and the slit domain Ω_S .

$$(57) \quad \Omega := (0, 1)^2, \quad \Omega_S := (-1, 1)^2 \setminus (0, 1] \times \{0\}.$$

In the *first test case* we study the Poisson equation over the unit square Ω with the manufactured solution

$$(58) \quad u(x, y) = \exp(-100(x - 1/2)^2 - 100(y - 117/1000)^2)$$

and essential boundary conditions, chosen accordingly. In the *second test case* we solve the Poisson equation $-\Delta u = 1$ over the slit domain Ω_S with homogeneous Dirichlet boundary conditions. For our numerical experiments we have computed a reference solution on a very fine mesh. Qualitative pictures of the two test solutions are given in Figure 2. We note that the solution of the first test case is contained in $H^2(\Omega)$ whereas the solution of the second test case is contained in $H^{\frac{3}{2}}(\Omega_S)$.

In the sequel, the initial meshes for the primal finite element methods over Ω and Ω_S are cubical meshes of resolution 16×16 in the first-order case; we use a 15×15 mesh in the second-order case so that the resulting finite element space has the same dimension.

6.2. Efficiency of local flux reconstruction. As a first numerical experiment we present a short parameter study demonstrating the robustness of the proposed local flux reconstruction. We solve both problems with tensor product Lagrange elements of order one and two and compute a flux reconstruction in the Raviart-Thomas space of order two or three, respectively. We compute the flux reconstruction either by solving the adjoint mixed problem or by patch-wise flux reconstruction. The efficiency $I_{\text{eff},f}$ of the respective equilibrated error estimate with reconstructed flux σ_h is assessed with the ratio in Equation (16).

Table 1 gives computational results for first and second order Lagrange elements. In the first test case with a manufactured solution, the efficiency indices of both methods of flux reconstruction are close to optimal, i.e., $I_{\text{eff},f} \approx 1$. That the data of the problem are not cellwise polynomial is reflected in the slight underestimation of the error in initial phases for the flux reconstruction via mixed methods. Both estimators appear to be asymptotically exact; we attribute this to the high regularity of ∇u and the higher polynomial order of the flux reconstruction, which make the term $\nabla u - \sigma$ converge to zero faster than $\nabla u - \nabla u_h$.

In the second test case over the slit domain, the efficiency is generally worse with $I_{\text{eff},f} \approx 1.5 - 3.0$ for the tested refinement levels. We attribute this to the corner singularity limiting the regularity of ∇u . We now also observe the predicted lower efficiency with local instead of global flux reconstruction (see Inequality (32)) and the effect of increased generic constants for higher polynomial order.

6.3. Energy-Oriented Adaptive Refinement. Additionally, the equilibrated error estimator has been tested in the second test case as a driver for adaptive mesh refinement. The local indicators are computed in accordance with (28), once with the flux reconstructed from a mixed finite element method and once with the locally reconstructed flux. We use a *fixed fraction* marking strategy where in each refinement step the 33% of cells with highest indicator values are marked for refinement. Table 2 displays the results with first-order Lagrange elements. The

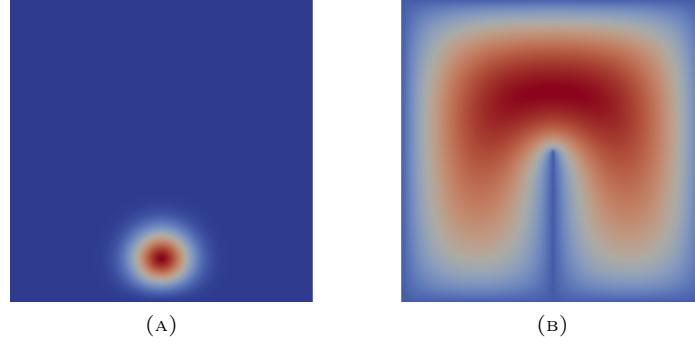


FIGURE 2. The two considered test cases. Picture (a) shows the manufactured solution (58) on the unit square, Picture (b) shows the solution on the slit domain with constant unit right hand side.

	#Dofs	$\ \nabla u_h - \nabla u\ _A^2$		Mixed method		Flux reconstruction	
				$\ \nabla u_h - \sigma_h\ _A^2$	$I_{\text{eff},f}$	$\ \nabla u_h - \sigma_h\ _A^2$	$I_{\text{eff},f}$
1	289	2.84e-4	0.97	2.62e-4	0.921	2.97e-4	1.047
2	1089	7.35e-5	1.95	7.20e-5	0.980	7.54e-5	1.026
3	4225	1.85e-5	1.99	1.85e-5	0.996	1.87e-5	1.009
4	16641	4.63e-6	2.00	4.64e-6	1.003	4.66e-6	1.006
5	66049	1.15e-6	2.02	1.16e-6	1.016	1.16e-6	1.017
1	289	2.11e-4	1.81	1.75e-4	0.830	1.85e-4	0.880
2	1089	1.02e-5	4.37	9.67e-6	0.953	1.03e-5	1.017
3	4225	6.69e-7	3.92	6.61e-7	0.988	6.76e-7	1.010
4	16641	4.24e-8	3.98	4.23e-8	0.997	4.26e-8	1.003
5	66049	2.66e-9	3.99	2.66e-9	0.999	2.66e-9	1.001

(A) Manufactured solution, first and second order

	#Dofs	$\ \nabla u_h - \nabla u\ _A^2$		Mixed method		Flux reconstruction	
				$\ \nabla u_h - \sigma_h\ _A^2$	$I_{\text{eff},f}$	$\ \nabla u_h - \sigma_h\ _A^2$	$I_{\text{eff},f}$
1	1105	2.46e-4	1.34	3.09e-4	1.255	3.99e-4	1.617
2	4257	1.06e-4	1.22	1.39e-4	1.309	1.83e-4	1.725
3	16705	4.76e-5	1.16	6.55e-5	1.376	8.73e-5	1.835
4	66177	2.14e-5	1.16	3.18e-5	1.488	4.26e-5	1.997
5	263425	8.96e-6	1.25	1.56e-5	1.745	2.11e-5	2.351
1	1105	1.19e-4	1.03	1.82e-4	1.529	2.75e-4	2.314
2	4257	5.82e-5	1.03	9.05e-5	1.556	1.37e-4	2.349
3	16705	2.81e-5	1.05	4.52e-5	1.609	6.82e-5	2.425
4	66177	1.31e-5	1.10	2.26e-5	1.723	3.41e-5	2.597
5	263425	5.62e-6	1.22	1.13e-5	2.011	1.70e-5	3.031

(B) Slit domain, first and second order

TABLE 1. Parameter study demonstrating the efficiency of the equilibrated error estimator for the two considered test cases of a manufactured solution (a) and a solution over the slit domain (b).

#Dofs				Mixed method		Flux reconstruction	
	$\ \nabla u_h - \nabla u\ _A^2$			$\ \nabla u_h - \sigma_h\ _A^2$	$I_{\text{eff},f}$	$\ \nabla u_h - \sigma_h\ _A^2$	$I_{\text{eff},f}$
1	311	4.80e-4	1.20	5.44e-4	1.132	6.32e-4	1.315
2	628	2.82e-4	0.77	3.16e-4	1.118	3.58e-4	1.270
3	1159	1.27e-4	1.16	1.45e-4	1.142	1.65e-4	1.304
4	2333	6.97e-5	0.86	8.02e-5	1.150	9.07e-5	1.302
5	4393	3.05e-5	1.19	3.72e-5	1.219	4.23e-5	1.388

TABLE 2. Parameter study demonstrating the efficiency of the local flux reconstruction for the second test case of a slit domain.

obtained efficiency indices $I_{\text{eff},f} \approx 1.4$ are considerably better than the corresponding case with uniform refinement (see Table 1). The estimator based on the local flux reconstruction has slightly worse efficiency indices but performs similarly well as the estimator based on the mixed method.

6.4. Goal-Oriented Error Estimation. Our next computational experiments assess the performance of our proposed goal-oriented error estimators. We consider the error approximations and indicators

$$\begin{aligned} \eta^{\varrho\varpi} &= \sum_{K \in \Omega_h} \eta_K^{\varrho\varpi}, & \eta_K^{\varrho\varpi} &= \int_K \langle \varrho_h, \varpi_h \rangle_A, \\ \eta^{\text{II},*} &= \sum_{K \in \Omega_h} \eta_K^{\text{II},*}, & \eta_K^{\text{II},*} &= \int_K \langle \varrho_h, z_h^* - z_h \rangle_A, \\ \eta^{\varrho\tau} &= \sum_{K \in \Omega_h} \eta_K^{\varrho\tau}, & \eta_K^{\varrho\tau} &= \int_K \langle \varrho_h, \tau_h \rangle_A. \end{aligned}$$

The error indicators $\eta^{\varrho\varpi}$ and $\eta^{\varrho\tau}$ utilize the local flux reconstructions in the primal and the dual problems. The error indicator $\eta^{\text{II},*}$ uses only the local flux reconstruction of the primal problem but employs an approximation z_h^* of the dual solution that is reconstructed by a well-known postprocessing technique—a patch-wise higher-order interpolation to a coarser mesh, $z_h^* = \Pi_{2h}^{(2r)} z_h$ in the notation of [9].

Whenever $\eta^* = \sum_{K \in \Omega_h} \eta_K^*$ is one of the error estimators with local indicators proposed in Section 5, we define the *efficiency index* I_{eff} and the *oscillation index* $I_{\text{osc}} \geq 1$ by

$$(59) \quad I_{\text{eff}} := \frac{|\eta^*|}{|J(u) - J(u_h)|}, \quad I_{\text{osc}} := \frac{1}{|\eta^*|} \left(\sum_{K \in \Omega_h} |\eta_K^*| \right).$$

Whereas I_{eff} measures the total efficiency of the error estimate, the quantity I_{osc} measures the oscillatory behavior of the local indicators. For our computational experiments we extend the two different test cases by goal functionals. Specifically, the quantity of interest is defined by small regularized point evaluations at $(0.5, 0.117)$ in the first case and at $(0.25, 0.75)$ in the second test case.

We have assessed the performance of the error approximations and indicators under uniform refinement, again considering first and second order Lagrange elements. For the sake of brevity we consider only the (practically interesting) case of local flux reconstruction.

(A) Manufactured solution, first and second order

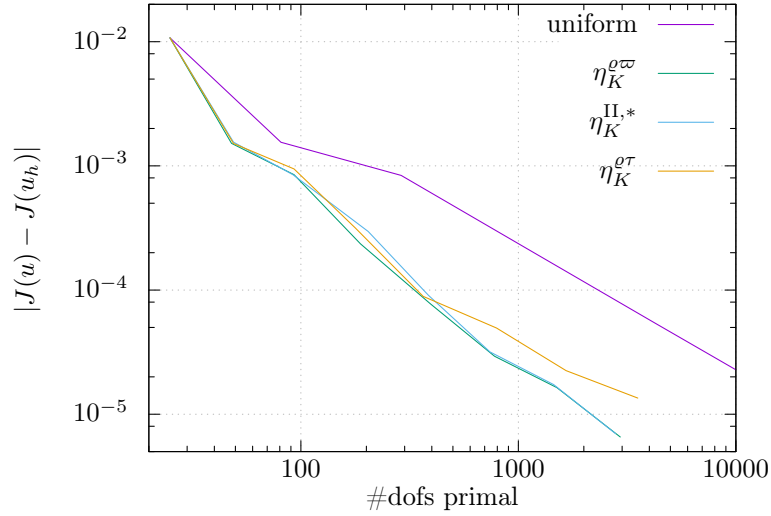
#Dofs	$ J(u) - J(u_h) $	$\eta^{e\varpi}$		$\eta^{II,*}$		$\eta^{e\tau}$			
		I_{eff}	I_{osc}	I_{eff}	I_{osc}	I_{eff}	I_{osc}		
1	289	8.38e-4	0.89	1.043	1.185	0.274	2.704	2.699	1.122
2	1089	2.17e-4	1.95	1.022	1.183	0.899	1.229	2.831	1.211
3	4225	5.45e-5	1.99	1.007	1.198	0.976	1.213	2.827	1.242
4	16641	1.36e-5	2.00	1.006	1.201	0.997	1.205	2.832	1.257
5	66049	3.37e-6	2.02	1.016	1.202	1.014	1.203	2.865	1.260
1	289	5.65e-4	2.06	0.893	1.000	0.183	1.265	0.462	2.440
2	1089	2.22e-5	4.67	1.021	1.001	1.242	1.001	1.936	4.089
3	4225	1.43e-6	3.95	1.008	1.044	0.903	1.081	1.965	5.601
4	16641	9.15e-8	3.96	0.989	1.049	0.985	1.057	1.941	5.923
5	66049	5.64e-9	4.02	1.003	1.047	1.030	1.051	1.974	6.037

(B) Slit domain, first and second order

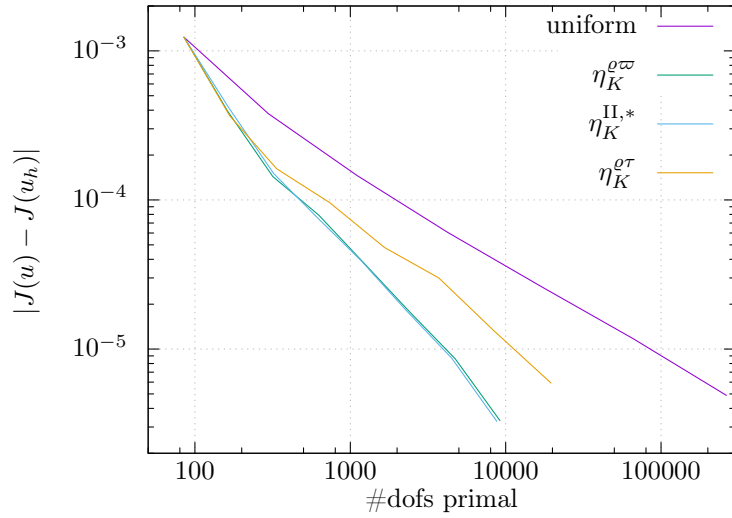
#Dofs	$ J(u) - J(u_h) $	$\eta^{e\varpi}$		$\eta^{II,*}$		$\eta^{e\tau}$			
		I_{eff}	I_{osc}	I_{eff}	I_{osc}	I_{eff}	I_{osc}		
1	1105	3.08e-4	1.29	1.639	1.015	0.454	1.062	1.284	1.126
2	4257	1.38e-4	1.16	1.699	1.008	0.391	1.041	1.308	1.111
3	16705	6.51e-5	1.08	1.733	1.004	0.354	1.023	1.321	1.107
4	66177	3.17e-5	1.04	1.746	1.002	0.333	1.014	1.322	1.105
5	263425	1.58e-5	1.01	1.739	1.001	0.319	1.008	1.313	1.105
1	1105	1.57e-4	0.92	2.164	1.001	0.115	1.093	1.836	1.709
2	4257	7.88e-5	0.99	2.045	1.000	0.108	1.066	1.736	1.706
3	16705	3.95e-5	1.00	1.859	1.000	0.099	1.063	1.578	1.710
4	66177	1.99e-5	0.99	1.572	1.000	0.083	1.062	1.334	1.715
5	263425	1.01e-5	0.98	1.201	1.000	0.064	1.062	1.019	1.718

TABLE 3. Efficiency I_{eff} and oscillatory behavior I_{osc} of different error estimators for first and second polynomial order and for the two test cases of (a) a manufactured solution on the unit square and (b) a solution on the slit-domain.

The results are given in Table 3. The proposed error approximation $\eta^{e\varpi}$ performs very well and appears to behave asymptotically exact in both test cases and both polynomial orders. By comparison, the error approximation $\eta^{II,*}$, which coincides with the error approximation of the dual weighted residual method (see Remark 14), performs reasonably on sufficiently fine meshes in the first (regular) test case but fails to approximate the true error in the second test case over the slit domain. The third error indicator $\eta^{e\tau}$ gives reliable upper bounds in the experiments but consistently overestimates the error in the regular first test case when compared to $\eta^{e\varpi}$ and $\eta^{II,*}$. Finally, it is worth mentioning that $\eta^{e\tau}$ consistently exhibits a pronounced oscillatory behavior whereas the oscillation index of $\eta^{e\varpi}$ and $\eta^{II,*}$ appear to be asymptotically optimal or near-optimal, respectively.



(A) unit square



(B) slit domain

FIGURE 3. Performance plot; error in the quantity of interest $|J(u) - J(u_h)|$ plotted over total number of primal degrees of freedoms for (a) the model problem on the unit square and (b) the model problem on the slit domain. Results for lowest-order, linear finite elements.

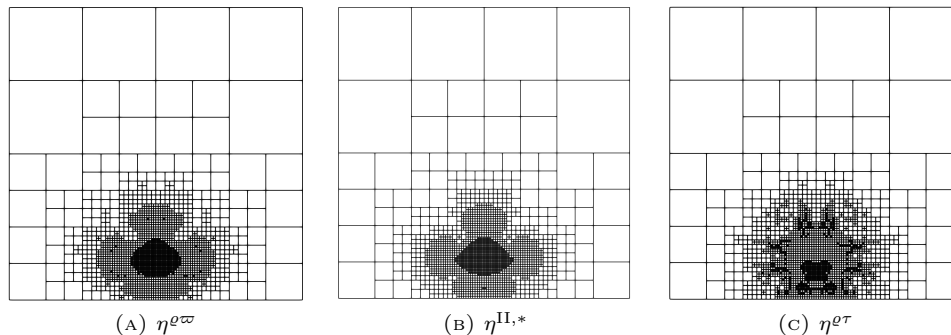


FIGURE 4. Resulting locally refined meshes obtained by different local indicators for the test case defined on the unit square. The unbalanced, oscillatory nature of $\eta^{e\tau}$ causes significant spurious refinement.

6.5. Goal-Oriented Estimator Competition. We conclude with testing the performance of the local indicators for adaptive refinement with lowest order Lagrange elements. Again, the local smoothed Dirac deltas are the goal functionals. Figure 3 shows a “performance plot” (error over number of primal degrees of freedom). All local indicators perform qualitatively better than uniform refinement. In both test cases, the two indicators $\eta^{e\infty}$ and $\eta^{II,*}$ perform optimally, i.e., with linear order of convergence. The indicator variant $\eta^{e\tau}$, however, leads to suboptimal asymptotic behavior. We attribute this to the oscillatory behavior, i.e., to “unbalanced” local indicators (see Table 3). Figure 4 displays the final locally refined meshes for visual comparison. The spurious refinement caused by the oscillatory nature of the indicator $\eta^{e\tau}$ is clearly visible.

7. CONCLUSION

The nature of our results is both experimental and theoretical.

Equilibrated error estimators have been implemented with the software library deal.II [5]. As a theoretical foundation we have discussed the construction and well-posedness of local flux reconstruction problems over quadrilateral meshes with hanging nodes (see Lemma 1). Techniques inspired by commuting interpolators have been used, the bulk of which have only been discussed for conforming simplicial meshes in the literature so far. Our computational experiments show uniformly bounded efficiency indices for all tested polynomial orders. The experimental observation that the localized flux reconstruction leads to competitive error estimates when compared to flux reconstruction via mixed finite element methods is corroborated by the inverse inequality (32). To the best of our knowledge, this is the first time this experimental observation has been traced to a rigorous estimate. We emphasize that the efficiency of the equilibrated error estimate can be understood best through convergence estimates for mixed finite element methods.

Our practical main results target the goal-oriented error estimation. The proposed error estimator $\eta^{e\infty}$ shows efficiency indices in the range 0.9 – 2.0, depending on the regularity of the domain, and its oscillation index is very well controlled by

1.2. This distinguishes it from the dual weighted residual method, which typically requires sufficiently fine meshes and higher problem regularity. Furthermore, our local indicators $\eta_K^{o\varpi}$ shows advantages over the error indicators $\eta_K^{o\tau}$, whose high oscillation index points to their suboptimal marking in goal-oriented adaptive finite element methods. We therefore recommend the indicators $\eta_K^{o\varpi}$ for adaptive marking and error estimation in the quantity of interest at the cost of numerically solving both the primal and the dual problem and performing a localized flux reconstruction for both.

REFERENCES

1. Mark Ainsworth, Leszek Demkowicz, and Chang-Wan Kim, *Analysis of the equilibrated residual method for a posteriori error estimation on meshes with hanging nodes*, Computer Methods in Applied Mechanics and Engineering **196** (2007), no. 37, 3493–3507.
2. Mark Ainsworth and J. Tinsley Oden, *A unified approach to a posteriori error estimation using element residual methods*, Numerische Mathematik **65** (1993), no. 1, 23–50.
3. ———, *A posteriori error estimation in finite element analysis*, vol. 37, John Wiley & Sons, 2011.
4. Mario Arioli, Jörg Liesen, Agnieszka Międlar, and Zdeněk Strakoš, *Interplay between discretization and algebraic computation in adaptive numerical solution of elliptic pde problems*, GAMM-Mitteilungen **36** (2013), no. 1, 102–129.
5. Daniel Arndt, Wolfgang Bangerth, Denis Davydov, Timo Heister, Luca Heltai, Martin Kronbichler, Matthias Maier, Bruno Turcksin, and David Wells, *The deal.II library, version 8.5*, Journal of Numerical Mathematics **in press** (2017).
6. Douglas N. Arnold, Daniele Boffi, and Francesca Bonizzoni, *Finite element differential forms on curvilinear cubic meshes and their approximation properties*, Numerische Mathematik **129** (2015), no. 1, 1–20.
7. Randolph E. Bank and Alan Weiser, *Some a posteriori error estimators for elliptic partial differential equations*, Mathematics of computation **44** (1985), no. 170, 283–301.
8. Roland Becker and Rolf Rannacher, *An optimal control approach to a posteriori error estimation in finite element methods*, Acta Numerica 2001 **10** (2001), 1–102.
9. Malte Braack and Thomas Richter, *Solutions of 3d navier-stokes benchmark problems with adaptive finite elements*, Computers and Fluids **35** (2006), 27–392.
10. Dietrich Braess, *Finite elements: Theory, fast solvers, and applications in solid mechanics*, Cambridge University Press, 2007.
11. Dietrich Braess, Thomas Fraunholz, and Ronald HW Hoppe, *An equilibrated a posteriori error estimator for the interior penalty discontinuous galerkin method*, SIAM Journal on Numerical Analysis **52** (2014), no. 4, 2121–2136.
12. Dietrich Braess, Veronika Pillwein, and Joachim Schöberl, *Equilibrated residual error estimates are p-robust*, Computer Methods in Applied Mechanics and Engineering **198** (2009), no. 13-14, 1189–1197.
13. Dietrich Braess and Joachim Schöberl, *Equilibrated residual error estimator for edge elements*, Mathematics of Computation **77** (2008), no. 262, 651–672.
14. Franco Brezzi and Michel Fortin, *Mixed and hybrid finite element methods*, vol. 15, Springer Science & Business Media, 2012.
15. Carsten Carstensen and Jun Hu, *Hanging nodes in the unifying theory of a posteriori finite element error control*, J. Comput. Math **27** (2009), no. 2-3, 215–236.
16. Carsten Carstensen and Christian Merdon, *Effective postprocessing for equilibration a posteriori error estimators*, Numerische Mathematik **123** (2013), no. 3, 425–459.
17. Timothy A. Davis, Patrick R. Amestoy, Iain S. Duff, et al., *SuiteSparse 4.2.1, A Suite of Sparse Matrix Software*, 2013.
18. Michael Feischl, Dirk Praetorius, and Kristoffer G. Van der Zee, *An abstract analysis of optimal goal-oriented adaptivity*, SIAM Journal on Numerical Analysis **54** (2016), no. 3, 1423–1448.
19. D. W. Kelly, *The self-equilibration of residuals and complementary a posteriori error estimates in the finite element method*, International Journal for Numerical Methods in Engineering **20** (1984), no. 8, 1491–1506.

20. Fumio Kikuchi and Hironobu Saito, *Remarks on a posteriori error estimation for finite element solutions*, Journal of computational and applied mathematics **199** (2007), no. 2, 329–336.
21. Kwang-Yeon Kim, *Postprocessing for guaranteed error bound based on equilibrated fluxes*, J. Korean Math. Soc **52** (2015), no. 5, 891–906.
22. Pierre Ladeveze and Dominique Leguillon, *Error estimate procedure in the finite element method and applications*, SIAM Journal on Numerical Analysis **20** (1983), no. 3, 485–509.
23. Robert Luce and Barbara I. Wohlmuth, *A local a posteriori error estimator based on equilibrated fluxes*, SIAM Journal on Numerical Analysis **42** (2004), no. 4, 1394–1414.
24. Pedro Morin, Ricardo Nochetto, and Kunibert Siebert, *Local problems on stars: a posteriori error estimators, convergence, and performance*, Mathematics of Computation **72** (2003), no. 243, 1067–1097.
25. Igor Mozolevski and Serge Prudhomme, *Goal-oriented error estimation based on equilibrated-flux reconstruction for finite element approximations of elliptic problems*, Computer Methods in Applied Mechanics and Engineering **288** (2015), 127–145.
26. Ricardo Nochetto, Andreas Veiser, and Marco Verani, *A safeguarded dual weighted residual method*, IMA journal of Numerical Analysis **29** (2008), no. 1, 126–140.
27. Dirk Pauly, *On Maxwell's and Poincaré's constants.*, Discrete & Continuous Dynamical Systems-Series S **8** (2015), no. 3.
28. Dirk Pauly and Sergei Repin, *Functional a posteriori error estimates for elliptic problems in exterior domains*, Journal of Mathematical Sciences **162** (2009), no. 3, 393–406.
29. William Prager and John L. Synge, *Approximations in elasticity based on the concept of function space*, Quarterly of Applied Mathematics **5** (1947), no. 3, 241–269.
30. Sergey I. Repin, *A posteriori estimates for partial differential equations*, vol. 4, Walter de Gruyter, 2008.
31. Tomáš Vejchodský, *Guaranteed and locally computable a posteriori error estimate*, IMA Journal of Numerical Analysis **26** (2006), no. 3, 525–540.
32. Tomáš Vejchodský, *Local a posteriori error estimator based on the hypercircle method*, Proceedings of the European Congress on Computational Methods in Applied Sciences and Engineering (ECCOMAS 2004), Jyväskylä, Finland, 2004.
33. Rüdiger Verfürth, *A note on constant-free a posteriori error estimates*, SIAM J. Numer. Anal **47** (2009), no. 4, 3180–3194.
34. Rüdiger Verfürth, *A posteriori error estimation techniques for finite element methods*, OUP Oxford, 2013.

UCSD DEPARTMENT OF MATHEMATICS, 9500 GILMAN DRIVE MC0112, LA JOLLA, CA 92093-0112, USA

E-mail address: `mlicht@ucsd.edu`

SCHOOL OF MATHEMATICS, UNIVERSITY OF MINNESOTA, MINNEAPOLIS, MINNESOTA 55455, USA

E-mail address: `msmaier@umn.edu`